



TITLE:

Spontaneous Hall effect in a chiral p-wave superconductor

AUTHOR(S):

Furusaki, A; Matsumoto, M; Sigrist, M

CITATION:

Furusaki, A ...[et al]. Spontaneous Hall effect in a chiral p-wave superconductor. PHYSICAL REVIEW B 2001, 64(5): 054514.

ISSUE DATE:

2001-08-01

URL:

<http://hdl.handle.net/2433/50454>

RIGHT:

Copyright 2001 American Physical Society

Spontaneous Hall effect in a chiral p -wave superconductor

Akira Furusaki,¹ Masashige Matsumoto,² and Manfred Sigrist^{1,*}

¹*Yukawa Institute for Theoretical Physics, Kyoto University, Kyoto 606-8502, Japan*

²*Department of Physics, Shizuoka University, Shizuoka 422-8529, Japan*

(Received 8 February 2001; published 12 July 2001)

In a chiral superconductor with broken time-reversal symmetry a “spontaneous Hall effect” may be observed. We analyze this phenomenon by taking into account the surface properties of a chiral superconductor. We identify two main contributions to the spontaneous Hall effect. One contribution originates from the Bernoulli (or Lorentz) force due to spontaneous currents running along the surfaces of the superconductor. The other contribution has a topological origin and is related to the intrinsic angular momentum of Cooper pairs. The latter can be described in terms of a Chern-Simons-like term in the low-energy field theory of the superconductor and has some similarities with the quantum Hall effect. The spontaneous Hall effect in a chiral superconductor is, however, nonuniversal. Our analysis is based on three approaches to the problem: a self-consistent solution of the Bogoliubov–de Gennes equation, a generalized Ginzburg-Landau theory, and a hydrodynamic formulation. All three methods consistently lead to the same conclusion that the spontaneous Hall resistance of a two-dimensional superconducting Hall bar is of order $h/(ek_F\lambda)^2$, where k_F is the Fermi wave vector and λ is the London penetration depth; the Hall resistance is substantially suppressed from a quantum unit of resistance. Experimental issues in measuring this effect are briefly discussed.

DOI: 10.1103/PhysRevB.64.054514

PACS number(s): 74.25.Fy, 74.25.Nf, 74.20.De, 74.70.Pq

I. INTRODUCTION

Unconventional superconductivity appears with a large variety of possible phases displaying many properties that are not shared by conventional s -wave superconductors. These phases are characterized by their symmetry properties, and in most cases not only the $U(1)$ -gauge symmetry but other symmetries are also spontaneously broken. Interesting physics emerges, in particular, when time-reversal symmetry \mathcal{T} is violated in a superconductor. Volovik and Gor'kov have classified such superconducting states into two categories, the so-called “ferromagnetic” and the “antiferromagnetic” states.¹ They are distinguished by the internal angular momentum of Cooper pairs. In the ferromagnetic state the Cooper pairs possess either a finite orbital or (for nonunitary states) spin moment, while in the antiferromagnetic state they have no net moments. Examples of these two types of states were recently discussed in connection with high-temperature superconductors; the so-called $d_{x^2-y^2} + id_{xy}$ -wave state represents a ferromagnetic pairing state, while the $d_{x^2-y^2} + is$ -wave state is antiferromagnetic. In high-temperature superconductors a \mathcal{T} -violating state is most likely to be realized only near surfaces or interfaces at very low temperatures.^{2–4} Among the heavy fermion superconductors there are two well-known systems which have \mathcal{T} -violating bulk superconducting phases: UPT_3 and $U_{1-x}Th_xBe_{13}$ ($0.017 < x < 0.45$). These materials show superconducting double transitions, and \mathcal{T} violation is associated with the second of the two transitions.⁵ A more recent candidate for \mathcal{T} -violating superconductivity is Sr_2RuO_4 ,⁶ a layered perovskite compound. Experimentally, Sr_2RuO_4 shows clear features of a strongly correlated quasi-two-dimensional Fermi liquid above the onset temperature of superconductivity $T_c = 1.5$ K. It was suggested⁷ that, since this system in the normal state behaves as a two-dimensional analogue to 3He , the superconducting phase would corre-

spond to the superfluid A phase, which is a well-known \mathcal{T} -violating pairing state.^{8–10} Indeed, the experimental evidence^{11,12} for unconventional superconductivity in Sr_2RuO_4 is consistent with the basic order parameter symmetry^{11–13}

$$\mathbf{d}(\mathbf{k}) = \hat{z}\Delta \frac{k_x \pm ik_y}{k_F}, \quad (1.1)$$

a p -wave (spin-triplet) state. Here we have used the standard notation of the \mathbf{d} vector to represent the order parameter of the triplet state⁸ $\hat{\Delta}(\mathbf{k}) = i\mathbf{d}(\mathbf{k}) \cdot \boldsymbol{\sigma}\sigma^y$, where σ^i are the Pauli matrices. The \mathbf{d} vector (1.1) pointing along the z direction implies that the spin part of the Cooper pair wave function is the spin-triplet state with $S_z = 0$, i.e., in-plane equal-spin pairing (the z direction is along the c axis of Sr_2RuO_4). In a system with cylindrical symmetry the orbital part of the pair wave function is a state with finite angular momentum along the z axis $L_z = \pm 1$. Obviously the state represented by Eq. (1.1) is “ferromagnetic,” and is also called chiral p -wave state.

The chirality of this superconducting state is characterized by a topological number N defined by^{9,10}

$$N = \frac{1}{4\pi} \int_{-\infty}^{\infty} dk_x \int_{-\infty}^{\infty} dk_y \hat{\mathbf{m}} \cdot \left(\frac{\partial \hat{\mathbf{m}}}{\partial k_x} \times \frac{\partial \hat{\mathbf{m}}}{\partial k_y} \right). \quad (1.2)$$

The unit vector $\hat{\mathbf{m}}(k_x, k_y)$ is

$$\hat{\mathbf{m}} = \frac{\mathbf{m}}{|\mathbf{m}|}, \quad \mathbf{m} = (\text{Re } d_z, \text{Im } d_z, \epsilon_k), \quad (1.3)$$

where $\epsilon_k = (k_x^2 + k_y^2)/2m - \mu$ is the kinetic energy measured from the chemical potential μ . (Throughout this paper we will assume the cylindrical symmetry whenever microscopic modeling is necessary, although the inclusion of crystal field

effects is straightforward. Note that, being topological, the number N can be defined without resorting to the cylindrical symmetry.) The topological number N corresponds to the multiplicity of the wrapping of a sphere S^2 in the mapping of $\mathbf{R}^2 \cup \{\infty\} \simeq S^2$ to another S^2 representing the unit vector $\hat{\mathbf{m}}$. The vector \mathbf{m} does not vanish at any \mathbf{k} , allowing us to define the topological number N uniquely. In the chiral p -wave state (1.1) the topological number N is either $+1$ or -1 depending on the chirality of the state or the orbital angular momentum.

A chiral superconductor has gapless chiral edge modes at interfaces between states of opposite chiralities (domain walls) or between a chiral state and a vacuum (surface), as dictated by the index theorem. Volovik pointed out¹⁰ that the topological invariant N determines the number of gapless edge modes per spin at a boundary between different states.¹⁰ This yields $2|N_1 - N_2|$ such modes at the interface of two domains characterized by the topological numbers N_1 and N_2 , respectively. At an interface between a chiral p -wave state and a vacuum we find two modes (one per spin). These states can be easily understood in terms of Andreev bound states.^{14–17} Recent point contact experiments provide the first indication for these states at the surface of Sr_2RuO_4 .¹⁸

The presence of gapless chiral edge modes is reminiscent of quantum Hall fluids. One can thus expect a chiral superconductor to have a Hall effect. This is a spontaneous Hall effect (SHE) in the sense that a transverse voltage appears in response to an external current even without an external magnetic field applied to the superconductor.⁹ The Hall conductance is not quantized, however, contrary to a naive analogy. This is because the electric current can be carried as a supercurrent by superconducting condensate or, in other words, the local charge density is not a conserved quantity in a superconductor.^{19–21} In fact, it has been shown^{20–22} that the spin and the thermal Hall conductance are quantized to the topological number N in appropriate units. Even though it is nonuniversal, the spontaneous (charge) Hall effect is interesting in its own right because it is an effect which can be experimentally measured, in principle. Thus we would like to investigate in detail in this paper the origin and magnitude of the effect. To this end, it is necessary to understand what one would actually measure in an experiment trying to observe the SHE. Computing a diagram for the current-current correlation function in a bulk superconductor does not give a proper solution to this problem. On the contrary, we have to understand physics near a surface of a chiral superconductor, taking into account issues such as (1) the spatial variation of the order parameter near the surface, (2) the spontaneous current running along the surface of the chiral superconductor, and (3) screening effects for both magnetic field and electric field in the superconductor. We study the surface properties using three different approaches: a numerical self-consistent analysis of the Bogoliubov–de Gennes (BdG) equation, an extended Ginzburg–Landau (GL) theory with a scalar potential, and a phenomenological hydrodynamic formulation. We find that there are two basic contributions to the SHE. The first is the Bernoulli force due to spontaneous currents which flow near the surface. They are the consequence of the chiral surface states, but can also be under-

stood in terms of a transverse order parameter textures. Naturally they lead to a Hall response. The second originates from the intrinsic magnetic moment of the Cooper pairs in the chiral p -wave state. The former contribution is present in both chiral and nonchiral superconductors, since both can have spontaneous surface currents, while the latter contribution exists only in chiral superconductors. We therefore conclude that even a nonchiral (antiferromagnetic) T -violating superconductor can have a SHE.

The organization of this paper is as follows. In Sec. II we introduce a simple microscopic model for the chiral p -wave superconductor and solve the BdG equation self-consistently at zero temperature. In Sec. III we present the extended GL theory and derive basic equations. They are used in Sec. IV to analyze the SHE near T_c . In Sec. V we present parameters appearing in the extended GL theory obtained from a microscopic weak-coupling analysis. The GL theory is the basis to formulate an effective hydrodynamical theory presented in Sec. VI, which allows us to interpret and estimate the SHE in a simple way distinguishing the two contributions mentioned above. In Sec. VII we also demonstrate the SHE in the nonchiral $s + id$ -wave state by the numerical BdG approach. The results are summarized in Sec. VIII.

II. SELF-CONSISTENT BOGOLIUBOV-DE GENNES ANALYSIS

A. Model formulation

We consider a chiral p -wave superconductor in which energy band and order parameter have no momentum dependence in the z direction. We may thus treat the system as if it is two dimensional. The starting point of our analysis is a mean-field Hamiltonian for a two-dimensional spin-triplet superconductor with $\mathbf{d} \parallel \hat{z}$. The Hamiltonian is given by $H_{\text{MF}} = \int dx dy \mathcal{H}_{\text{MF}}$ with the Hamiltonian density

$$\begin{aligned} \mathcal{H}_{\text{MF}} = & \sum_{\sigma} \psi_{\sigma}^{\dagger}(\mathbf{r}) h_0(\mathbf{r}) \psi_{\sigma}(\mathbf{r}) + \frac{1}{g} |\boldsymbol{\eta}(\mathbf{r})|^2 \\ & - \frac{i}{2k_F} \{ \boldsymbol{\eta}(\mathbf{r}) \cdot [\psi_{\uparrow}^{\dagger}(\mathbf{r}) \nabla \psi_{\uparrow}^{\dagger}(\mathbf{r}) + \psi_{\downarrow}^{\dagger}(\mathbf{r}) \nabla \psi_{\downarrow}^{\dagger}(\mathbf{r})] \\ & + \boldsymbol{\eta}^*(\mathbf{r}) \cdot [\psi_{\downarrow}(\mathbf{r}) \nabla \psi_{\uparrow}(\mathbf{r}) + \psi_{\uparrow}(\mathbf{r}) \nabla \psi_{\downarrow}(\mathbf{r})] \}, \quad (2.1) \end{aligned}$$

$$h_0(\mathbf{r}) = \frac{1}{2m} \left[-i\hbar \nabla + \frac{e}{c} \mathbf{A}(\mathbf{r}) \right]^2 - \mu - eA_0(\mathbf{r}), \quad (2.2)$$

where ψ_{σ} is the annihilation operator of electron with spin $\sigma = \uparrow, \downarrow$, g is the coupling constant of the attractive interaction that is responsible for p -wave pairing ($g > 0$), and $\nabla = (\partial_x, \partial_y)$. The superconducting order parameter should satisfy the (self-consistence) gap equation, obtained from $(\delta/\delta \boldsymbol{\eta}^*) \langle H_{\text{MF}} \rangle = 0$,

$$\boldsymbol{\eta} = (\eta_x, \eta_y) = \frac{ig}{2k_F} \langle \psi_{\uparrow}(\mathbf{r}) [\nabla \psi_{\downarrow}(\mathbf{r})] - [\nabla \psi_{\uparrow}(\mathbf{r})] \psi_{\downarrow}(\mathbf{r}) \rangle. \quad (2.3)$$

We are interested in systems with boundaries in which the order parameter $\boldsymbol{\eta}$ depends on $\mathbf{r}=(x,y)$. The uniform system with \mathbf{d} given in Eq. (1.1) corresponds to the case $\boldsymbol{\eta}=\Delta(1, \pm i)$.

The equations of motion for the field ψ_σ are $i\hbar\partial_t\psi_\sigma=[\psi_\sigma, H_{\text{MF}}]$. Substituting $\psi_\uparrow=ue^{-i\epsilon t/\hbar}$ and $\psi_\downarrow=ve^{-i\epsilon t/\hbar}$ into them, we arrive at the BdG equation

$$h_0(\mathbf{r})u_n(\mathbf{r})-\frac{i}{2k_F}[\boldsymbol{\eta}\cdot\nabla v_n+\nabla\cdot(v_n\boldsymbol{\eta})]=\epsilon_n u_n(\mathbf{r}), \quad (2.4a)$$

$$-h_0^*(\mathbf{r})v_n(\mathbf{r})-\frac{i}{2k_F}[\boldsymbol{\eta}^*\cdot\nabla u_n+\nabla\cdot(u_n\boldsymbol{\eta}^*)]=\epsilon_n v_n(\mathbf{r}). \quad (2.4b)$$

The wave functions are normalized in two dimensions: $\int dx dy (|u_n|^2 + |v_n|^2) = 1$. When (u_n, v_n) is an eigenfunction with energy ϵ_n , (v_n^*, u_n^*) is an eigenstate with energy $-\epsilon_n$. With these eigenfunctions the field operators are expanded as

$$\begin{pmatrix} \psi_\uparrow(\mathbf{r}, t) \\ \psi_\downarrow(\mathbf{r}, t) \end{pmatrix} = \sum_{\epsilon_n \geq 0} \begin{pmatrix} u_n & v_n^* \\ v_n & u_n^* \end{pmatrix} \begin{pmatrix} \gamma_{n\uparrow} e^{-i\epsilon_n t/\hbar} \\ \gamma_{n\downarrow} e^{i\epsilon_n t/\hbar} \end{pmatrix}. \quad (2.5)$$

The ground state $|0\rangle$ satisfies $\gamma_{n\sigma}|0\rangle=0$.

Gapless chiral edge modes are present at boundaries of a chiral p -wave superconductor. To illustrate this within our model, it is sufficient to solve the BdG equation with a simplified gap function with step-function form, $\boldsymbol{\eta}=\Theta(x)\Delta(1, i\epsilon)$, where $\Theta(x)$ is the Heaviside step function and $\epsilon=\pm 1$ is the chirality of the condensate. The self-consistent solution of the BdG equation will be presented in the next subsection. The bound state solution to Eq. (2.4) with energy eigenvalue $\epsilon=\Delta\sin\theta$ ($-\pi/2<\theta<\pi/2$) and with boundary condition $u_n=v_n=0$ at $x=0$ is given by

$$\begin{pmatrix} u_\theta(\mathbf{r}) \\ v_\theta(\mathbf{r}) \end{pmatrix} = \sqrt{\frac{2}{\xi_0 L_y}} \exp\left(-\frac{x}{\xi_0} + i\epsilon k_F y \sin\theta\right) \sin(k_F x \cos\theta) \times \begin{pmatrix} e^{i\pi/4} \\ e^{-i\pi/4} \end{pmatrix}, \quad (2.6)$$

where L_y is a linear scale of the superconductor in y -direction. We have used the Andreev approximation valid for $\Delta \ll \mu$. The amplitude of the edge state decays in the bulk on the length $\xi_0 = \hbar v_F / \Delta$. With the wave number in the y direction $k_y = \epsilon k_F \sin\theta$, the energy dispersion of the chiral edge mode is $\epsilon(k_y) = \epsilon \Delta k_y / k_F$.

We now calculate current carried by the chiral edge mode at zero temperature. The current density \mathbf{J} is defined as

$$\begin{aligned} J_i &= -c \frac{\delta}{\delta A_i} \int d^2 r \mathcal{H}_{\text{MF}} \\ &= -e \sum_\sigma \left\{ \frac{\hbar}{2im} [\psi_\sigma^\dagger (\partial_i \psi_\sigma) - (\partial_i \psi_\sigma^\dagger) \psi_\sigma] + \frac{e}{mc} A_i \psi_\sigma^\dagger \psi_\sigma \right\}, \end{aligned} \quad (2.7)$$

where the fields ψ_σ are expanded as in Eq. (2.5). At this level a finite contribution comes only from the edge mode (2.6). Thus, we may restrict the summation over the eigenstates to $0 < \theta < \pi/2$. The total charge current running along the edge is given by

$$\begin{aligned} I_y &= \int_0^\infty dx \langle 0 | J_y | 0 \rangle \\ &= -\frac{e\hbar}{m} \int_0^\infty dx \text{Im} \langle 0 | \psi_\uparrow^\dagger \partial_y \psi_\uparrow + \psi_\downarrow^\dagger \partial_y \psi_\downarrow | 0 \rangle \\ &= -\frac{2e\hbar}{m} \frac{k_F L_y}{2\pi} \int_0^1 d(\sin\theta) \int_0^\infty dx \text{Im}(v_\theta \partial_y v_\theta^*) = \frac{\epsilon e \mu}{2\pi\hbar}, \end{aligned} \quad (2.8)$$

where we have set $A=0$, ignoring the vector potential induced by the spontaneous current, i.e., diamagnetic screening currents. The current I_y is spontaneously running along the edge of the chiral p -wave superconductor. If the chemical potential could be shifted by a constant as $\mu \rightarrow \mu + eV$ in some way, then the spontaneous current would change by $\epsilon e^2 V / h$. From this simple-minded argument it is tempting to conclude a universal value of the Hall conductance. This argumentation is invalid, because both the superconducting condensate and the edge states carry current and, furthermore, the constant shift of the chemical potential is not realistic to describe a Hall measurement. Indeed a careful analysis of the physics of the superconductor surface region is necessary as we will demonstrate below.

B. Solution for Hall bar geometry

In this section we study the transverse voltage induced by an externally driven current by solving the BdG equations (2.4) self-consistently for a system with Hall bar geometry. We model the Hall bar by a two-dimensional system of width L_x in the x direction and length L_y in the y direction. The currents run along the y direction, in which we impose the periodic boundary conditions. The superconducting state with the symmetry of the chiral p -wave state is parametrized by $\boldsymbol{\eta}=(\Delta_x, i\Delta_y)$, where Δ_x and Δ_y are real functions of \mathbf{r} . The calculation is done for zero temperature.

In the Hall bar geometry it is convenient to use the following two basis sets of wave functions

$$\begin{pmatrix} \psi_{\sin}(\mathbf{k}, \mathbf{r}) \\ \psi_{\cos}(\mathbf{k}, \mathbf{r}) \end{pmatrix} = \sqrt{\frac{2}{L_x L_y}} e^{ik_y y} \begin{pmatrix} \sin k_x x \\ \cos k_x x \end{pmatrix}, \quad (2.9)$$

where $k_y = 2l\pi/L_y$ and $k_x = m\pi/L_x$ (l, m : integer) by setting either the wave function or its first derivative to zero at x

$=0$ and L_x . We solve the problem twice: (i) with the Dirichlet boundary condition at $x=0$ and L_x and (ii) with the Neumann boundary condition. Afterwards we take the average of both solutions in order to remove unphysically rapid changes of the electron density at the surface. Expanding $u_n(\mathbf{r})$ and $v_n(\mathbf{r})$ as

$$\begin{pmatrix} u_n(\mathbf{r}) \\ v_n(\mathbf{r}) \end{pmatrix} = \sum_{\mathbf{k}} \begin{pmatrix} \tilde{u}_n(\mathbf{k}) \\ \tilde{v}_n(\mathbf{k}) \end{pmatrix} \psi_{\sin, \cos}(\mathbf{k}, \mathbf{r}), \quad (2.10)$$

we can solve the gap equation numerically by diagonalization. The order parameter is determined self-consistently from the gap equation (2.3) for $T=0$

$$(\Delta_x, i\Delta_y) = \frac{ig}{2k_F} \sum_{E_n > 0} [u_n(\mathbf{r}) \nabla v_n^*(\mathbf{r}) - v_n^*(\mathbf{r}) \nabla u_n(\mathbf{r})], \quad (2.11)$$

where the coupling constant g is chosen to give $\Delta_x = \Delta_y = \Delta_0$ in a bulk chiral p -wave superconductor. Thus, g is obtained by solving the gap equation

$$\begin{aligned} \frac{1}{g} &= \frac{1}{(4\pi k_F)^2} \int d^2k \frac{k^2}{\sqrt{\epsilon_k^2 + (\Delta_0 k/k_F)^2}} \\ &= \frac{m}{8\pi\hbar^2} \int_{-\omega_c}^{\omega_c} d\epsilon \frac{1 + \epsilon/\mu}{\sqrt{\epsilon^2 + \Delta_0^2(1 + \epsilon/\mu)}} = \frac{m}{8\pi\hbar^2} (I_1 + I_2), \end{aligned} \quad (2.12)$$

where ω_c is a cutoff energy and

$$\begin{aligned} I_1 &= \int_{-\omega_c}^{\omega_c} d\epsilon \frac{1}{\sqrt{\epsilon^2 + \Delta_0^2(1 + \epsilon/\mu)}} \\ &= \ln \left| \frac{2\omega_c + \Delta_0^2/\mu + 2\sqrt{\omega_c^2 + \Delta_0^2(1 + \omega_c/\mu)}}{-2\omega_c + \Delta_0^2/\mu + 2\sqrt{\omega_c^2 + \Delta_0^2(1 - \omega_c/\mu)}} \right|, \\ I_2 &= \frac{1}{\mu} \int_{-\omega_c}^{\omega_c} d\epsilon \frac{\epsilon}{\sqrt{\epsilon^2 + \Delta_0^2(1 + \epsilon/\mu)}} \\ &= \frac{1}{\mu} \left[\sqrt{\omega_c^2 + \Delta_0^2 \left(1 + \frac{\omega_c}{\mu}\right)} - \sqrt{\omega_c^2 + \Delta_0^2 \left(1 - \frac{\omega_c}{\mu}\right)} \right] \\ &\quad - \frac{\Delta_0^2 I_1}{2\mu^2}. \end{aligned}$$

The solutions to the BdG equation (2.4) determine the electron density and current density

$$n_e(\mathbf{r}) = 2 \sum_{E_n > 0} |v_n(\mathbf{r})|^2, \quad (2.13a)$$

$$\begin{aligned} J_y(\mathbf{r}) &= \frac{ie\hbar}{m} \sum_{E_n > 0} \left[v_n(\mathbf{r}) \frac{\partial v_n^*(\mathbf{r})}{\partial y} - v_n^*(\mathbf{r}) \frac{\partial v_n(\mathbf{r})}{\partial y} \right] \\ &\quad - \frac{e^2}{mc} n_e(\mathbf{r}) A_y(\mathbf{r}), \end{aligned} \quad (2.13b)$$

where only the y component of the current is nonvanishing in the Hall bar geometry. Note that these densities are defined in two dimensions because of the normalization condition imposed on u_n and v_n . The scalar and vector potentials obey the Maxwell equations

$$\nabla^2 A_0(\mathbf{r}) = -\frac{4\pi e}{d} [n_b - n_e(\mathbf{r})], \quad \nabla^2 A_y(\mathbf{r}) = -\frac{4\pi}{cd} J_y(\mathbf{r}). \quad (2.14)$$

We have introduced the length d to convert the area densities into the volume densities. Physically d corresponds to the spacing between two-dimensional layers in Sr_2RuO_4 . To keep overall charge neutrality, we introduce n_b as the density of the uniform positive background charge (jellium model). The externally injected current I fixes the boundary conditions for the vector potential

$$\left. \frac{\partial A_y}{\partial x} \right|_{x=0} = -\left. \frac{\partial A_y}{\partial x} \right|_{x=L_x} = \frac{2\pi}{cd} I. \quad (2.15)$$

The self-consistent order parameters, scalar and vector potentials can be obtained numerically by solving Eqs. (2.4), (2.11), and (2.14) iteratively until convergence is reached. In the iteration step we fix the total number of electrons to the normal state value by adjusting μ . In the self-consistent solution electric charge is screened on the Thomas-Fermi length scale $l = (\hbar^2 d / 4e^2 m)^{1/2}$. Since we have three material-dependent parameters Δ_0 , k_F , and d , we have freedom to change three dimensionless parameters $k_F \xi_0$, λ / ξ_0 , and l / ξ_0 .

C. Discussion of the self-consistent solution

The solutions of the BdG equation reveal that the relevant physics of the Hall bar indeed happens at the two surfaces. First we consider the solution for the case where total current along the y direction is zero. The order parameter varies strongly at the surface: Δ_x is suppressed while Δ_y rises slightly as shown in Fig. 1(a). This behavior is connected with the reflection properties of Cooper pairs at the surface. Resulting interference effects are destructive for Δ_x , since the order parameter is odd under reflection at a surface normal to the x direction. Note that this order parameter variation is specific for a specular reflection at the surface and would look different for the case of diffuse scattering. We do not, however, consider this aspect here further.

At the surface the chiral edge states appear with a linear dispersion around the Fermi energy. These are Andreev bound states as a direct consequence of the chirality of the superconducting state. The two branches seen in Fig. 1(b) belong each to one of the two edges of the bar. These chiral edge states generate spontaneous currents at the surface flowing along $\mathbf{n} \times \hat{\mathbf{z}}$ (\mathbf{n} : surface normal vector). The currents on the two edges of the Hall bar run in opposite directions,

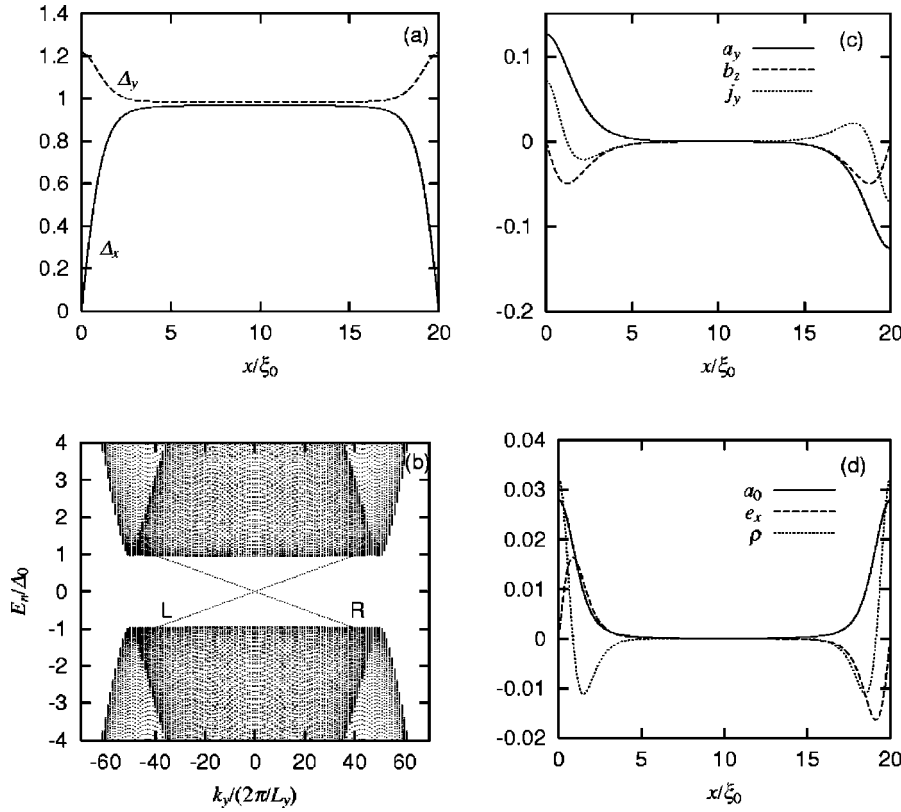


FIG. 1. Self-consistent solution of the Bogoliubov-de Gennes equation of the $p_x + ip_y$ -wave state at $T=0$. The set of parameters are chosen as $\xi_0 = \hbar v_F / \Delta_0$, $k_F \xi_0 = 16$, $\omega_c = 8\Delta_0$, $\kappa = \lambda / \xi_0 = 1$, $l = 0.25\xi_0$, and $L_x = L_y = 20\xi_0$. (a) Order parameter scaled by Δ_0 , which is the magnitude of the order parameter in the bulk region. (b) Energy eigenvalues obtained for sine basis functions. L and R denote the surface bound states localized near $x=0$ and $x=L_x$, respectively. States with $|E_n| > \Delta_0$ are extended. Unit of k_y is $2\pi/L_y$. (c) Dimensionless vector potential $a_y = (e\xi_0/\hbar c)A_y$, magnetic field $b_z = \xi_0 \partial_x a_y$, and current density $j_y = -\xi_0 \partial_x b_z$. (d) Dimensionless scalar potential $a_0 = eA_0/\Delta_0$, electric field $e_x = -\xi_0 \partial_x a_0$, and charge density $\rho = \xi_0 \partial_x e_x$.

thereby no net current is flowing in the Hall bar. The edge currents generate a magnetic field, which is screened by counter currents in the interior of the superconductor [Fig. 1(c)]. The length scale of the surface current is the coherence length ξ_0 while the screening currents spread over the London penetration depth λ . The surface magnetic fields generate a finite magnetization whose sign depends on the sign of Cooper pair angular momentum and the sign of the charge, i.e., electronlike or holelike Fermi surface.

Turning now to the question of the scalar potential and the charge distribution in the superconductor, we find again that all interesting features show up only in the surface region. There is a finite excess charge at the surface, which is screened due to Thomas-Fermi screening. As a result the charge density forms a dipole layer and is overall charge neutral. This is the constraint that we have imposed by fixing the external electrical field to zero (note that in our Hall bar geometry a finite charge or equivalently a finite external electric field would correspond to an infinite field energy, since the capacitance is zero). The dipole layer induces a local electric field and causes a shift of the scalar potential relative to its value in the bulk of the superconductor which we choose to be zero. The charge distributions and potential at the surface are the same on both sides of the bar.

Under the assumption that the Hall bar is symmetric about $x=L_x/2$, there is no potential difference between the two sides. We would like to mention that scalar potential variations close to the surface are not unique to chiral superconducting states, but occur in any superconductor whose order parameter is influenced by surface scattering.

If we introduce a net current driven from an external source, this external current will be distributed equally to both surfaces [see Fig. 2(a)]. This affects the surface states differently for the two sides, because on one side the external current flows with the spontaneous current, on the other against it. Furthermore, the scalar potential is not equal anymore at the two sides because the charge dipole layers are modified differently, as we can see in Fig. 2(b). This transverse voltage difference depends on the orientation of the external current and appears in the absence of an external magnetic field.

Our calculation clearly shows a linear relation between the source current I and the transverse voltage V_H as expected for the Hall effect. Deviations occur only when the current approaches the critical value where the order parameter starts to be strongly affected by the current. In Fig. 3 we show the κ , l , and $k_F \xi_0$ dependences of the Hall resistance $R_H = V_H/I$. What is immediately obvious is that the Hall resistance is strongly suppressed from the quantum unit of resistance $R_0 = h/2e^2$. There is also a strong dependence on the material dependent parameters, indicating that the behavior is nonuniversal. Unfortunately, in the numerical BdG scheme we are limited in the choice of l , ξ_0 , λ , and k_F^{-1} , because large difference in their magnitudes demands large-scale computation. In the next section we study the SHE using the extended GL theory which will allow us to calculate R_H analytically for temperatures close to T_c . We can already here confirm that the quantitative comparison between the two methods works very well. It will also become clear that there are a few contributions to the transverse voltage.

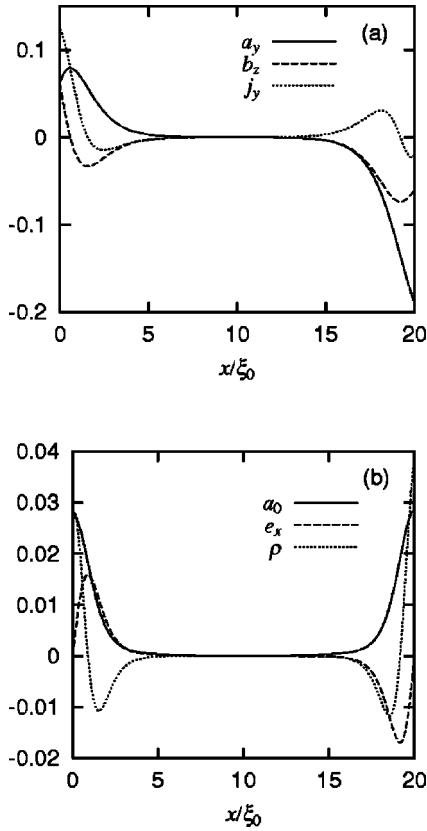


FIG. 2. Self-consistent solution of the Bogoliubov-de Gennes equation at $T=0$ when current $I=5e\Delta_0/\hbar k_F\xi_0$ is externally supplied. Set of parameters are the same as used in Fig. 1. (a) Dimensionless vector potential, magnetic field, and current density. (b) Dimensionless scalar potential, electric field, and charge density.

III. GINZBURG-LANDAU FORMULATION

We formulate an extended Ginzburg-Landau theory based on symmetry arguments which includes the scalar and vector potentials in a general form. This allows us to analyze the anomalous coupling between charge and magnetic degrees of freedom in chiral superconductors.

A. Ginzburg-Landau free energy

The paring symmetry of the chiral p -wave superconducting state is characterized by $\mathbf{d}(\mathbf{k}) = \hat{\mathbf{z}}\Delta(k_x \pm ik_y)/k_F$, which is a combination of the two degenerate p -wave components with p_x and p_y symmetry. This degeneracy is not lifted when we introduce a tetragonal crystal field, although the details of the k dependence of \mathbf{d} may change. The twofold degeneracy requires that we introduce two complex order parameter components $\boldsymbol{\eta} = (\eta_x, \eta_y)$, such that the \mathbf{d} vector becomes $\mathbf{d}(\mathbf{k}) = \hat{\mathbf{z}}(\boldsymbol{\eta} \cdot \mathbf{k})/k_F$. The free energy has to be a scalar under the transformations of the symmetry group

$$\mathcal{G} = D_{4h} \times T \times U(1), \quad (3.1)$$

where the tetragonal point group D_{4h} includes the simultaneous transformation of orbital and spin degree of freedom as a consequence of spin-orbit coupling, T denotes the time-

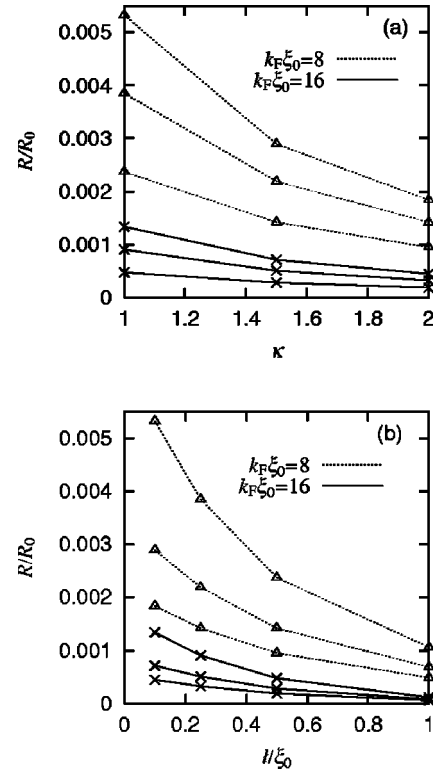


FIG. 3. (a) κ dependence of the Hall resistance. Within the same $k_F\xi_0$, the three lines from the top correspond to $l=0.1\xi_0$, $l=0.25\xi_0$, and $l=0.5\xi_0$, respectively. (b) l dependence of the Hall resistance. Within the same $k_F\xi_0$, three lines from the top correspond to $\kappa=1$, $\kappa=1.5$, and $\kappa=2$, respectively. In both figures the Hall resistance R is scaled by $R_0 = h/2e^2$.

reversal symmetry and $U(1)$ the gauge symmetry. The GL free energy expansion for $\boldsymbol{\eta}$ with the symmetry \mathcal{G} is well known:²³ $F = \int d^3r \mathcal{F}$, where

$$\begin{aligned} \mathcal{F} = & a \boldsymbol{\eta} \cdot \boldsymbol{\eta}^* + b_1 (\boldsymbol{\eta} \cdot \boldsymbol{\eta}^*)^2 + \frac{b_2}{2} (\eta_x^{*2} \eta_y^2 + \eta_x^2 \eta_y^{*2}) \\ & + b_3 |\eta_x|^2 |\eta_y|^2 + K_1 (|D_x \eta_x|^2 + |D_y \eta_y|^2) \\ & + K_2 (|D_x \eta_y|^2 + |D_y \eta_x|^2) + K_3 [(D_x \eta_x)^* (D_y \eta_y) + \text{c.c.}] \\ & + K_4 [(D_x \eta_y)^* (D_y \eta_x) + \text{c.c.}] + K_5 (|D_z \eta_x|^2 + |D_z \eta_y|^2) \\ & + \frac{(\nabla \times \mathbf{A})^2}{8\pi}. \end{aligned} \quad (3.2)$$

The coefficients a , b_i , and K_i are nonuniversal real numbers that depend on the details of the material. The coefficient a is negative below T_c ($a \propto T - T_c$). For the choice $0 < b_2 < 4b_1 + b_3$ and $b_3 < b_2$, we find the homogeneous phase $\boldsymbol{\eta} = \eta_0(1, \pm i)$ with $\eta_0^2(T) = |a|/(4b_1 - b_2 + b_3)$. The gradient terms are explicitly gauge invariant by the definition $\mathbf{D} = \nabla + i(2e/\hbar c)\mathbf{A}$. Equation (3.2) is the standard free energy density used to study the response to the magnetic field with the Coulomb gauge $\nabla \cdot \mathbf{A} = 0$.

As is well known,²⁴ the intrinsic orbital angular momentum in a chiral p -wave state is related to the difference of the two terms with coefficients K_3 and K_4 :

$$(D_x \eta_x)^* D_y \eta_y - (D_x \eta_y)^* D_y \eta_x + \text{c.c.} \\ = \left[\nabla \times (\eta_x^* \mathbf{D} \eta_y - \eta_y^* \mathbf{D} \eta_x) \right. \\ \left. + i \frac{2e}{\hbar c} (\eta_y^* \eta_x - \eta_x^* \eta_y) \nabla \times \mathbf{A} \right]_z, \quad (3.3)$$

where it is understood that the z component of a three-dimensional vector is kept in the right-hand side. The integral of the first term gives a surface term which we may

discard, while the second term represents the Zeeman energy of a magnetic moment coming from the intrinsic angular momentum ($\propto i \boldsymbol{\eta} \times \boldsymbol{\eta}^*$).

For our purpose it is essential to include additional terms that are coupled to either the scalar potential A_0 or the electric field $\mathbf{E} = -\nabla A_0$. We consider the stationary situation and fix the gauge so that A_0 is zero in the undisturbed homogeneous superconductor. It is more convenient to use the Lagrangian formulation, in which the Maxwell equations simply follow from variation with respect to A_μ . The Lagrangian density involving the scalar potential is given by

$$\mathcal{L}_e = \tilde{K}_1 A_0 (|D_x \eta_x|^2 + |D_y \eta_y|^2) + \tilde{K}_2 A_0 (|D_x \eta_y|^2 + |D_y \eta_x|^2) + \tilde{K}_3 A_0 [(D_x \eta_x)^* (D_y \eta_y) + (D_x \eta_x) (D_y \eta_y)^*] \\ + \tilde{K}_4 A_0 [(D_x \eta_y)^* (D_y \eta_x) + (D_x \eta_y) (D_y \eta_x)^*] + \tilde{K}_5 A_0 (|D_z \eta_x|^2 + |D_z \eta_y|^2) + C_1 [E_x \eta_x^* (D_x \eta_x) + E_y \eta_y^* (D_y \eta_y) + \text{c.c.}] \\ + C_2 [E_x \eta_y^* (D_x \eta_y) + E_y \eta_x^* (D_y \eta_x) + \text{c.c.}] + C_3 [E_x \eta_x^* (D_y \eta_y) + E_y \eta_y^* (D_x \eta_x) + \text{c.c.}] \\ + C_4 [E_x \eta_y^* (D_y \eta_x) + E_y \eta_x^* (D_x \eta_y) + \text{c.c.}] + C_5 [E_z \eta_x^* (D_z \eta_x) + E_z \eta_y^* (D_z \eta_y) + \text{c.c.}] - \frac{(\nabla A_0)^2}{8\pi} - \frac{A_0^2}{8\pi l^2} \quad (3.4)$$

with \tilde{K}_i, C_i , and l being real numbers. The coefficients will be derived for the weak-coupling limit in Sec. V. In this form it is easy to verify that each term is individually invariant. The term $A_0^2/8\pi l^2$ describes the screening of the electric charge in the metallic and superconducting state, where l is the Thomas-Fermi screening length. The choice of this form fixes A_0 to zero in the bulk of the superconductors, which corresponds to the chemical potential as required by our choice of gauge. We emphasize that $\mathcal{L}_e + \mathcal{F}$ plays a role of the Lagrangian density for A_μ .

We notice that the \tilde{K}_i terms are closely related with the K_i terms. On the other hand, the C_i terms have no relatives in Eq. (3.2). The difference of the C_3 and C_4 terms contains a contribution $i(\eta_x \eta_y^* - \eta_y \eta_x^*)(A_x \partial_y A_0 - A_y \partial_x A_0)$. It describes a coupling between the scalar and the vector potentials and is similar to the Chern-Simons (CS) term. Since the fields are static, however, it is not exactly the same as the CS term. Thus we shall call it a CS-like term. It can also be

interpreted as representing a coupling between the intrinsic magnetic moment ($\propto i \boldsymbol{\eta} \times \boldsymbol{\eta}^*$) and the magnetic field in the presence of an electric field. In other words, the CS-like term describes the reaction of the intrinsic magnetic moment to a change in the Cooper pair density.²⁵ The CS-like term proportional to $C_3 - C_4$ will play an essential role in the SHE, in addition to others.

B. Equations for the electromagnetism

We derive equations describing the electromagnetic properties of the superconductor from variation of $\int d^3r (\mathcal{L}_e + \mathcal{F})$ with respect to A_0 and \mathbf{A} . The equation for the scalar potential has the form

$$-\nabla^2 A_0 + \frac{A_0}{l^2} = 4\pi [\tilde{\rho} - \nabla \cdot (\mathbf{P} + \boldsymbol{\Pi})], \quad (3.5)$$

where

$$\tilde{\rho} = \tilde{K}_1 (|D_x \eta_x|^2 + |D_y \eta_y|^2) + \tilde{K}_2 (|D_x \eta_y|^2 + |D_y \eta_x|^2) + \tilde{K}_3 [(D_x \eta_x)^* (D_y \eta_y) + (D_x \eta_x) (D_y \eta_y)^*] \\ + \tilde{K}_4 [(D_x \eta_y)^* (D_y \eta_x) + (D_x \eta_y) (D_y \eta_x)^*] + \tilde{K}_5 (|D_z \eta_x|^2 + |D_z \eta_y|^2), \quad (3.6a)$$

$$\mathbf{P} = - \left(\begin{array}{c} \partial_x (C_1 |\eta_x|^2 + C_2 |\eta_y|^2) + \frac{1}{2} (C_3 + C_4) \partial_y (\eta_x^* \eta_y + \eta_x \eta_y^*) \\ \partial_y (C_1 |\eta_y|^2 + C_2 |\eta_x|^2) + \frac{1}{2} (C_3 + C_4) \partial_x (\eta_x^* \eta_y + \eta_x \eta_y^*) \\ C_5 \partial_z |\boldsymbol{\eta}|^2 \end{array} \right), \quad (3.6b)$$

$$\mathbf{\Pi} = \frac{1}{2} (C_3 - C_4) \begin{pmatrix} \eta_y^* D_y \eta_x + \eta_y D_y^* \eta_x^* - \eta_x^* D_y \eta_y - \eta_x D_y^* \eta_y^* \\ \eta_x^* D_x \eta_y + \eta_x D_x^* \eta_y^* - \eta_y^* D_x \eta_x - \eta_y D_x^* \eta_x^* \\ 0 \end{pmatrix}. \quad (3.6c)$$

The two terms on the left-hand side of Eq. (3.5) describe the screening of the electric field. The quantity $\tilde{\rho}$ is the charge density induced by variations of the order parameter. The vector density \mathbf{P} represents the electric polarization caused by inhomogeneities of the superconducting condensate. Both $\tilde{\rho}$ and \mathbf{P} appear as a consequence of the fact that the local change in the condensate, both in the order parameter and in the supercurrent, leads to a redistribution of the electric charge. This is most easily seen in $\tilde{\rho}$, which is related to the gradient term of the free energy. Note that terms of this kind are also present in conventional superconductors. On the other hand, the vector density $\mathbf{\Pi}$ is anomalous and characteristic of chiral superconductors.

For the sake of simplicity we assume that the relative phase of the order parameter component is fixed, i.e., $\eta_x = |\eta_x| \exp(i\phi)$ and $\eta_y = i\varepsilon |\eta_y| \exp(i\phi)$ with $\varepsilon = \pm 1$, where ε is the chirality of the p -wave order parameter. This condition is satisfied in the situations we will study below. In this case we have $i(\eta_y^* \eta_x - \eta_x^* \eta_y) = 2\varepsilon |\eta_x| |\eta_y|$. The vector $\mathbf{\Pi}$ can be written as

$$\mathbf{\Pi} = 2\varepsilon (C_3 - C_4) |\eta_x| |\eta_y| \left(\nabla \phi + \frac{2e}{\hbar c} \mathbf{A} \right) \times \hat{\mathbf{z}}. \quad (3.7)$$

Its divergence is equivalent to a source charge

$$\begin{aligned} \rho_{\Pi} &= -\nabla \cdot \mathbf{\Pi} \\ &= -\frac{4e}{\hbar c} \varepsilon |\eta_x| |\eta_y| B_z (C_3 - C_4) \\ &\quad - 2\varepsilon (C_3 - C_4) (\nabla |\eta_x| |\eta_y|) \times \left(\nabla \phi + \frac{2e}{\hbar c} \mathbf{A} \right). \end{aligned} \quad (3.8)$$

The first term indicates that the magnetic field B induces the electric charge whose sign depends on the chirality ε . The second term is nonvanishing only when the modulus of the order parameter has spatial variation. Terms similar to the latter also exist in $\tilde{\rho}$.

The modified London equation is obtained by variation of $\int d^3r (\mathcal{L}_e + \mathcal{F})$ with respect to \mathbf{A} :

$$\nabla^2 \mathbf{A} + \frac{4\pi}{c} (\mathbf{J} + \tilde{\mathbf{J}} + \mathbf{Y}) = 0, \quad (3.9)$$

where we find three current contributions. The first two,

$$\mathbf{J} = -\frac{4e}{\hbar} \begin{pmatrix} \text{Im}(K_1 \eta_x^* D_x \eta_x + K_2 \eta_y^* D_x \eta_y + K_3 \eta_x^* D_y \eta_y + K_4 \eta_y^* D_y \eta_x) \\ \text{Im}(K_1 \eta_y^* D_y \eta_y + K_2 \eta_x^* D_y \eta_x + K_3 \eta_y^* D_x \eta_x + K_4 \eta_x^* D_x \eta_y) \\ \text{Im}(K_5 \eta_x^* D_z \eta_x + K_5 \eta_y^* D_z \eta_y) \end{pmatrix} \quad (3.10a)$$

and

$$\tilde{\mathbf{J}} = -A_0 \frac{4e}{\hbar} \begin{pmatrix} \text{Im}(\tilde{K}_1 \eta_x^* D_x \eta_x + \tilde{K}_2 \eta_y^* D_x \eta_y + \tilde{K}_3 \eta_x^* D_y \eta_y + \tilde{K}_4 \eta_y^* D_y \eta_x) \\ \text{Im}(\tilde{K}_1 \eta_y^* D_y \eta_y + \tilde{K}_2 \eta_x^* D_y \eta_x + \tilde{K}_3 \eta_y^* D_x \eta_x + \tilde{K}_4 \eta_x^* D_x \eta_y) \\ \text{Im}(\tilde{K}_5 \eta_x^* D_z \eta_x + K_5 \eta_y^* D_z \eta_y) \end{pmatrix}, \quad (3.10b)$$

are the supercurrents including the screening currents. The second one contributes only if the scalar potential deviates from its bulk value $A_0 = 0$. The last term

$$\mathbf{Y} = i \frac{2e}{\hbar} (C_3 - C_4) (\eta_x \eta_y^* - \eta_x^* \eta_y) \mathbf{E} \times \hat{\mathbf{z}} \quad (3.10c)$$

is the anomalous contribution, where the electric field acts as a source of supercurrent. Note, however, that \mathbf{Y} does not

cause dissipation because $\mathbf{E} \cdot \mathbf{Y} = 0$. Both anomalous components $\mathbf{\Pi}$ and \mathbf{Y} are proportional to the chirality ε and originate from the CS-like term. We would like to emphasize here that the presence of the anomalous current contribution does not affect the standard flux quantization. The current \mathbf{Y} quickly drops to zero inside the superconducting material because the electrical field is strongly screened. Thus even a hole containing a net charge would not violate standard flux quantization.¹⁹

IV. TRANSVERSE VOLTAGE IN THE GL DESCRIPTION

Now we shall study the SHE in a Hall bar geometry on the level of the extended GL theory. Since we concluded in the BdG study that the relevant physics lies in the behavior of the superconductor close to the surface whose influence is exponentially small in the interior, we concentrate only on one edge and consider the half-space $x \geq 0$. The physics of a Hall bar of a given width L_x follows in a simple way from the results obtained for a single edge.

A. The surface state

The boundary conditions for the order parameter are chosen assuming specular surface scattering. For the given geometry they read

$$\eta_x|_{x=0}=0 \text{ and } D_x \eta_y|_{x=0}=0, \quad (4.1)$$

implying that there is no current running normal through the surface.²³ We need to consider only the x component of the electric field and the z component of the magnetic field, both of which are continuous at the surface and are functions of x . It can be easily shown that these boundary conditions are compatible with the gauge invariance of \mathcal{F}_e . The self-inductance L and the capacitance C of our system are taken to be infinity and zero, respectively, such that net current and total charge in the system should vanish, unless they are imposed by external sources. This is important for the choice of the boundary conditions for the gauge fields.

We present an approximate solution to the GL equation that captures the essential aspects of the problem. We assume that the system is in a chiral p -wave state of a single domain with the chirality ε . First we solve the GL equations to determine the spatial dependence of the order parameter η . To this end we ignore the gauge fields A_μ in the GL equation. This is allowed because we are looking for a solution in lowest order in $\tau = (T_c - T)/T_c$, a small parameter in the theory. The GL equations for $\eta_x = |\eta_x|$ and $\eta_y = i\varepsilon|\eta_y|$ are

$$K_1 \frac{d^2 |\eta_x|}{dx^2} = a|\eta_x| + 2b_1|\eta_x|^3 + (2b_1 - b_2 + b_3)|\eta_x||\eta_y|^2, \quad (4.2a)$$

$$K_2 \frac{d^2 |\eta_y|}{dx^2} = a|\eta_y| + 2b_1|\eta_y|^3 + (2b_1 - b_2 + b_3)|\eta_x|^2|\eta_y|. \quad (4.2b)$$

To simplify the analysis we consider a special situation where the coefficients b_i in the GL free energy satisfy the relation

$$2b_1 = b_2 - b_3, \quad (4.3)$$

which, however, is not satisfied for a cylindrical Fermi surface in the weak-coupling limit (see Sec. V). Under this condition Eqs. (4.2a) and (4.2b) have the solution

$$\eta_x = \eta_0 \tanh\left(\frac{x}{\xi}\right), \quad \eta_y = i\varepsilon \eta_0 \quad (4.4)$$

with $\eta_0^2 = |a|/2b_1$ and the coherence length $\xi^2 = 2K_1/|a|$. Note that η_x vanishes linearly at $x=0$ whereas η_y stays constant. If the condition (4.3) is not satisfied, η_y deviates slightly at $x \lesssim \xi$ from the bulk value η_0 , but generally does not vanish at $x=0$, as we have seen in the BdG study. In general the order parameter shows the following feature: the component of η normal to the surface vanishes linearly while the perpendicular component is only weakly affected. As the detailed spatial dependence of η is not important for our semiquantitative discussion, we will use an approximate form for η_x , instead of Eq. (4.4), which allows us to proceed with analytic calculations more easily,

$$\eta_x = \eta_0(1 - e^{-x/\xi}). \quad (4.5)$$

We would like to mention that we have solved the coupled GL equations for more general cases by numerical means to confirm that our approximations work very well both qualitatively and quantitatively.

Having determined the profile of the order parameter, we can calculate the distribution of the charge and the spontaneous current in the equilibrium state from Eqs. (3.6) and (3.10). The equations for the scalar and vector potential have the following form:

$$\begin{aligned} \frac{d^2 A_0}{dx^2} - \frac{A_0}{l^2} - \frac{\varepsilon}{l_1}(1 - e^{-x/\xi}) \frac{dA_y}{dx} - \frac{\varepsilon A_y}{\xi l_1 l_2} (l_1 + l_2) e^{-x/\xi} \\ + \frac{A_y^2}{e l_3(x)} = \frac{4\pi\eta_0^2}{\xi^2} [2C_1 e^{-x/\xi} - (4C_1 + \tilde{K}_1) e^{-2x/\xi}], \end{aligned} \quad (4.6)$$

$$\begin{aligned} \frac{d^2 A_y}{dx^2} - \frac{A_y}{\lambda^2} - \frac{\varepsilon}{l_1}(1 - e^{-x/\xi}) \frac{dA_0}{dx} + \frac{\varepsilon A_0}{\xi l_2} e^{-x/\xi} - \frac{2A_0 A_y}{e l_3(x)} \\ = -\varepsilon \frac{e}{\xi \lambda l_4} e^{-x/\xi}, \end{aligned} \quad (4.7)$$

where we have introduced parameters l_i ($i=1-4$) that have dimension of length

$$\frac{1}{l_1} = \frac{16\pi e \eta_0^2}{\hbar c} (C_3 - C_4), \quad (4.8a)$$

$$\frac{1}{l_2} = \frac{16\pi e \eta_0^2}{\hbar c} \tilde{K}_3, \quad (4.8b)$$

$$\frac{1}{l_3(x)} = \frac{16\pi e^3 \eta_0^2}{\hbar^2 c^2} [\tilde{K}_1 + \tilde{K}_2 (1 - e^{-x/\xi})^2], \quad (4.8c)$$

$$\frac{1}{l_4} = \frac{16\pi \eta_0^2 \lambda K_3}{\hbar c}. \quad (4.8d)$$

The London penetration depth λ is given by

$$\frac{1}{\lambda^2} = \frac{32\pi e^2 \eta_0^2}{\hbar^2 c^2} (K_1 + K_2). \quad (4.9)$$

In deriving Eq. (4.7) we have replaced

$$\frac{1}{\lambda^2} \left[1 - \frac{K_2}{K_1 + K_2} (2e^{-x/\xi} - e^{-2x/\xi}) \right]$$

by λ^{-2} ignoring the spatial dependence. This approximation weakly affects a numerical factor in the final expression of the Hall voltage.

For temperatures close to the onset of superconductivity, $\tau = (T_c - T)/T_c$ is a small parameter which allows for a controlled approximation. From the standard temperature dependence of η_0 , ξ , and λ , it is clear that

$$\frac{1}{l_i} = \mathcal{O}(\tau). \quad (4.10)$$

We first consider the case of vanishing external fields, i.e., $E=B=0$ in the vacuum ($x < 0$). This means that the net charge and current in the superconductor are zero. In this case the scalar potential $A_0^{(0)}$ and the vector potential $A_y^{(0)}$ obey the boundary conditions $dA_0^{(0)}/dx = dA_y^{(0)}/dx = 0$ at $x = 0$. From Eq. (4.10) we see that $A_0^{(0)} = \mathcal{O}(\tau^2)$ and $A_y^{(0)} = \mathcal{O}(\tau^{1/2})$ since $l = \mathcal{O}(\tau^0)$ and $l \ll \xi, \lambda$. In lowest order in τ we find

$$A_y^{(0)}(x) = \varepsilon \frac{e}{l_4} \frac{\kappa}{\kappa^2 - 1} (\kappa e^{-x/\lambda} - e^{-x/\xi}), \quad (4.11)$$

$$\begin{aligned} A_0^{(0)}(x) = & -l^2 \left\{ \frac{\varepsilon}{l_1} (1 - e^{-x/\xi}) \frac{dA_y^{(0)}(x)}{dx} \right. \\ & + \frac{\varepsilon}{\xi} \left(\frac{1}{l_1} + \frac{1}{l_2} \right) \left[A_y^{(0)}(x) e^{-x/\xi} - \frac{l}{\xi} A_y^{(0)}(0) e^{-x/l} \right] \\ & - \frac{1}{el_3(x)} [A_y^{(0)}(x)]^2 \\ & + \frac{4\pi\eta_0^2}{\xi^2} \left[2C_1 e^{-x/\xi} - (4C_1 + \tilde{K}_1) e^{-2x/\xi} \right. \\ & \left. \left. + \frac{2l}{\xi} (3C_1 + \tilde{K}_1) e^{-x/l} \right] \right\}, \end{aligned} \quad (4.12)$$

where $\kappa = \lambda/\xi$. This gives the total magnetic flux per length,

$$\Phi^{(0)} = \int_0^\infty dx B_z(x) = -A_y^{(0)}(0) = -\varepsilon \frac{e}{l_4} \frac{\kappa}{\kappa + 1}. \quad (4.13)$$

Note that the vector potential $A_y^{(0)}$ is proportional to ε whereas the scalar potential is independent of the chirality. For both the scalar and the vector potential the London penetration depth constitutes the longest length scale of variation, because they are coupled together. The charge density $-(1/4\pi)d^2A_0^{(0)}/dx^2$ has dipolar form as found in the BdG calculation. The total current density is

$$j_y^{(0)} = -\frac{c}{4\pi} \frac{d^2A_y^{(0)}(x)}{dx^2} = \varepsilon \frac{ce}{4\pi l_4 \lambda \xi} \frac{\kappa}{\kappa^2 - 1} (\kappa e^{-x/\xi} - e^{-x/\lambda}), \quad (4.14)$$

where the first term is related to the spontaneous current due to the chiral Andreev bound states, and the second term is the response of the superconductor, i.e., the screening current. Thus the net current is zero in the absence of an external magnetic field.

Results obtained for the semi-infinite geometry can be easily carried over to a Hall bar that extends from $x=0$ to $x=L_x$. When the width L_x of the Hall bar is much larger than λ , the two surfaces are basically disconnected electromagnetically. The gauge fields for the Hall bar geometry are then obtained by combining the contributions from the two edges. The scalar potential is $A_0^{(0)}(x) + A_0^{(0)}(L_x - x)$, while the vector potential is $A_y^{(0)}(x) - A_y^{(0)}(L_x - x)$.

B. Response to external fields

We now consider two cases where a weak external field is applied to the semi-infinite system. Weak perturbations introduce corrections to the gauge fields, $A_0 = A_0^{(0)} + \delta A_0$ and $A_y = A_y^{(0)} + \delta A_y$. We would like to obtain δA_μ in linear response to the external perturbation. We can, therefore, linearize the Maxwell equations in δA_μ :

$$\begin{aligned} \frac{d^2\delta A_0}{dx^2} - \frac{\delta A_0}{l^2} - \frac{\varepsilon}{l_1} (1 - e^{-x/\xi}) \frac{d\delta A_y}{dx} - \frac{\varepsilon}{\xi} \left(\frac{1}{l_1} + \frac{1}{l_2} \right) e^{-x/\xi} \delta A_y \\ + \frac{2A_y^{(0)}}{el_3(x)} \delta A_y = 0, \end{aligned} \quad (4.15)$$

$$\begin{aligned} \frac{d^2\delta A_y}{dx^2} - \frac{\delta A_y}{\lambda^2} - \frac{\varepsilon}{l_1} (1 - e^{-x/\xi}) \frac{d\delta A_0}{dx} + \frac{\varepsilon}{\xi l_2} e^{-x/\xi} \delta A_0 \\ - \frac{2}{el_3(x)} (A_0^{(0)} \delta A_y + A_y^{(0)} \delta A_0) = 0. \end{aligned} \quad (4.16)$$

(1) In the first case a weak external magnetic field $B\hat{z}$ is present in the vacuum, which corresponds to a finite net current running in the y direction. The boundary conditions are $d\delta A_0/dx = 0$ and $d\delta A_y/dx = B$ at $x = 0$. In leading orders in τ we obtain

$$\delta A_y^{(1)}(x) = -\lambda B e^{-x/\lambda}, \quad (4.17)$$

$$\begin{aligned} \delta A_0^{(1)}(x) = & -\varepsilon B l^2 \left\{ \frac{1}{l_1} \left[e^{-x/\lambda} (1 - e^{-x/\xi}) + \frac{l}{\xi} e^{-x/l} \right] \right. \\ & - \kappa \left(\frac{1}{l_1} + \frac{1}{l_2} \right) \left(e^{-x/\lambda - x/\xi} - \frac{l}{\xi} e^{-x/\lambda - x/l} \right) \\ & - \frac{l}{\lambda} e^{-x/l} \left. + \frac{2}{l_4} \frac{\kappa}{\kappa^2 - 1} \left[\frac{\lambda}{l_3(x)} e^{-x/\lambda} (\kappa e^{-x/\lambda} \right. \right. \right. \\ & \left. \left. - e^{-x/\xi}) - \frac{l}{l_3(0)} e^{-x/l} (\kappa - 1) \right] \right\}. \end{aligned} \quad (4.18)$$

We note that the sign of the scalar potential in linear response to B depends on the chirality ε .

This result can be used to determine the transverse voltage in the Hall bar. We assume that the induced current flows symmetrically on the two edges. Formally this situation is realized by applying the field $B\hat{z}[\Theta(-x) - \Theta(x - L_x)]$. The change of the scalar potential is $\delta A_0^{(1)}(x) - \delta A_0^{(1)}(L_x - x)$, leading to a finite transverse voltage across the Hall bar, $V_H = A_0(L_x) - A_0(0) = -2\delta A_0^{(1)}(0)$. Now we can make connection to the SHE in a two-dimensional system or in a layered system such as Sr_2RuO_4 , where the system consists of layers (xy planes) separated by a distance d . The total current per layer I is related to the external magnetic field by $I = c dB/2\pi$. From Eq. (4.18) we find

$$V_H = \varepsilon I \frac{4\pi l^2}{cd} \left[-\kappa \left(\frac{1}{l_1} + \frac{1}{l_2} \right) + \frac{2\lambda}{l_3(0)l_4} \frac{\kappa}{\kappa+1} \right], \quad (4.19)$$

where we have kept only the leading terms, which are proportional to τ . The parameters entering this expression will be derived from a microscopic model in the weak-coupling limit in the next section.

(2) We now turn to the second case where a weak external electric field $E\hat{x}$ is applied to the superconductor, inducing a finite surface charge. A similar problem was recently discussed by Goryo and Ishikawa.¹⁹ The boundary conditions here are $d\delta A_0/dx = -E$ and $d\delta A_y/dx = 0$ at $x=0$. In lowest orders in τ we find the solution to Eqs. (4.15) and (4.16),

$$\delta A_0^{(2)}(x) = El e^{-x/l}, \quad (4.20)$$

$$\begin{aligned} \delta A_y^{(2)}(x) \approx & -\varepsilon El^2 e^{-x/l} \left(\frac{x+2l}{l_1\xi} + \frac{l}{l_2\xi} - \frac{2l}{l_3(0)l_4} \frac{\kappa}{\kappa+1} \right) \\ & + \varepsilon El^2 e^{-x/\lambda} \left[\kappa \left(\frac{1}{l_1} + \frac{1}{l_2} \right) - \frac{2\lambda}{l_3(0)l_4} \frac{\kappa}{\kappa+1} \right]. \end{aligned} \quad (4.21)$$

The external electric field changes the local configuration of electric current and magnetic field in the chiral superconductor. The induced vector potential $\delta A_y^{(2)}$ depends on the chirality ε . The total change in the magnetic flux (per unit length along the y direction at the surface) is

$$\delta\Phi = -\delta A_y^{(2)}(0) = \varepsilon El^2 \left[-\kappa \left(\frac{1}{l_1} + \frac{1}{l_2} \right) + \frac{2\lambda}{l_3(0)l_4} \frac{\kappa}{\kappa+1} \right]. \quad (4.22)$$

Note the similarity between Eqs. (4.19) and (4.22) indicating that the two phenomena indeed have a common origin.

V. THE WEAK-COUPLING COEFFICIENTS OF THE GL THEORY

In this section we calculate the coefficients of the GL free energy in the weak-coupling limit using a model with layers of two-dimensional electron gas, where electrons are confined in each layer. Furthermore we ignore any spatial variation of electromagnetic fields in the direction perpendicular to the layers.

The mean-field Hamiltonian appropriate for the discussion of the chiral p -wave state (1.1) is already given in Eq. (2.1). The static electromagnetic fields are governed by

$$\mathcal{H}_{\text{EM}} = \frac{d}{8\pi} [(\nabla \times \mathbf{A})^2 - (\nabla A_0)^2], \quad (5.1)$$

where d is the distance between the two-dimensional layers. The sign of the second term was chosen negative so that the Maxwell equations can be obtained by taking the functional derivative of $\int d^2r (\mathcal{H}_{\text{MF}} + \mathcal{H}_{\text{EM}})$ with respect to A_μ , which should be viewed as the Lagrangian in imaginary time.

We integrate out the electron fields ψ_σ , and $\bar{\psi}_\sigma$ to obtain the effective functional F_{eff} for $\boldsymbol{\eta}$ and A_μ :

$$\begin{aligned} \exp(-F_{\text{eff}}/k_B T) = & \int \prod_\sigma \mathcal{D}\bar{\psi}_\sigma \mathcal{D}\psi_\sigma \\ & \times \exp \left[-\frac{1}{\hbar} \int_0^{\hbar/k_B T} dt \int d^2r (\hbar \bar{\psi}_\sigma \partial_t \psi_\sigma \right. \\ & \left. + \mathcal{H}_{\text{MF}} + \mathcal{H}_{\text{EM}}) \right], \end{aligned} \quad (5.2)$$

where the electron field operators $\psi_\sigma(\mathbf{r})$ and $\bar{\psi}_\sigma(\mathbf{r})$ in \mathcal{H}_{MF} (2.1) are replaced by Grassman fields $\psi_\sigma(\mathbf{r}, it)$ and $\bar{\psi}_\sigma(\mathbf{r}, it)$, respectively. The GL equations are then obtained by taking the functional derivative of F_{eff} with respect to $\boldsymbol{\eta}$ and A_μ . We calculate F_{eff} in powers of η_i and A_μ up to the order η_i^4 , $D_i \eta_j D_k \eta_l$, $A_0 D_i \eta_j D_k \eta_l$, and $E_i \eta_j D_k \eta_l$ in the weak-coupling limit, $|\boldsymbol{\eta}| \ll \hbar^2 k_F^2 / 2m$. The calculation is tedious but straightforward, and only the final result is presented below. The functional F_{eff} so obtained has the form

$$F_{\text{eff}} = \int d^3r (\mathcal{F} + \mathcal{L}_e). \quad (5.3)$$

The free energy part \mathcal{F} , which is defined in Eq. (3.2) as the free-energy density in *three* dimensions, has the standard coefficients

$$a = -\frac{\tau}{2} N(0), \quad (5.4a)$$

$$\frac{b_1}{3} = \frac{b_2}{2} = -\frac{b_3}{2} = \frac{7\zeta(3)N(0)}{128(\pi k_B T_c)^2}, \quad (5.4b)$$

$$\frac{K_1}{3} = K_2 = K_3 = K_4 = \frac{7\zeta(3)N(0)}{128} \left(\frac{\hbar v_F}{\pi k_B T_c} \right)^2, \quad (5.4c)$$

where T_c depends on the coupling constant g in the usual exponential form $k_B T_c = \omega_c \exp[-2/gN(0)]$ with ω_c being the cutoff energy scale, and $N(0) = m/(2\pi\hbar^2 d)$ is the density of states (per spin) at the Fermi level. The results (5.4) are valid in lowest order in $|\boldsymbol{\eta}|/\mu$, where we find $K_3 = K_4$. If we assume that the density of states had a weak energy dependence with energy derivative $N'(0) \approx N(0)/\mu$

$=m^2/(\pi\hbar^4k_F^2d)$ at the Fermi surface, then there would be a tiny difference between K_3 and K_4 , yielding the contribution to the free energy density

$$\begin{aligned}\mathcal{F}_Z &= \frac{e\hbar N'(0)}{8cm} \ln\left(\frac{2e^C\omega_D}{\pi T_c}\right) [i\boldsymbol{\eta}(\mathbf{r}) \times \boldsymbol{\eta}^*(\mathbf{r})] \cdot \mathbf{B} \\ &= -\frac{n_0\eta_0^2}{2\mu^2} \ln\left(\frac{2e^C\omega_D}{\pi T_c}\right) \boldsymbol{\mu} \cdot \mathbf{B},\end{aligned}\quad (5.5)$$

where $C=0.5772\dots$ is the Euler's constant, $n_0=k_F^2/2\pi d$ is the electron density, and $\boldsymbol{\mu}$ is the magnetic moment (per electron) of a Cooper pair in the chiral p -wave state

$$\boldsymbol{\mu} = -\hat{z} \frac{\mu_B}{2\eta_0^2} \text{Im}(\eta_x^* \eta_y). \quad (5.6)$$

Here $\mu_B=e\hbar/2mc$ is the Bohr magneton. Equation (5.5) is the Zeeman energy for the intrinsic magnetic moment of the chiral p -wave state. As is well known,²⁵⁻²⁷ it is diminished by the factor $(\eta_0/\mu)^2$ which indicates the degree of particle-hole asymmetry at the Fermi level. Since this contribution is very small, we can ignore it in the following analysis.

From the coefficients in Eq. (5.4) we immediately obtain the order parameter

$$\eta_0(T) = \pi k_B T_c \sqrt{\frac{8\tau}{7\xi(3)}}, \quad (5.7)$$

the coherence length

$$\xi(T) = \sqrt{\frac{2K_1}{|a|}} = \frac{\hbar v_F}{\pi k_B T_c} \sqrt{\frac{21\xi(3)}{32\tau}}, \quad (5.8)$$

and the London penetration depth

$$\lambda(T) = \frac{\hbar c}{2e\eta_0} \sqrt{\frac{1}{8\pi(K_1+K_2)}} = \frac{c}{ev_F} \sqrt{\frac{1}{8\pi\tau N(0)}}. \quad (5.9)$$

The second contribution to the free energy \mathcal{L}_e has the following coefficients:

$$\frac{1}{8\pi l^2} = e^2 N(0), \quad (5.10a)$$

$$\frac{\tilde{K}_1}{3} = \tilde{K}_2 = \tilde{K}_3 = \tilde{K}_4 = \frac{7\xi(3)e}{128\pi d(\pi k_B T_c)^2}, \quad (5.10b)$$

$$-C_1 = C_2 = -\frac{C_3}{3} = C_4 = \frac{7\xi(3)e}{256\pi d(\pi k_B T_c)^2}. \quad (5.10c)$$

Notice that $\tilde{K}_i = e\partial K_i/\partial\mu$. This relation can be easily understood, if we regard eA_0 as a spatial variation of μ . In the course of deriving Eqs. (5.10b) and (5.10c) we have naturally assumed that the momentum \mathbf{k} in $\mathbf{d}(\mathbf{k}) = \hat{z}(\boldsymbol{\eta} \cdot \mathbf{k})/k_F$ is close to the Fermi surface. The CS-like term describing the reaction of the intrinsic magnetic moment to a change in the

superfluid density does *not* have the reduction factor found in Eq. (5.5), in agreement with the argument by Volovik and Mineev.^{25,28}

From Eqs. (5.4) and (5.10) we obtain the parameters appearing in Eqs. (4.19) and (4.22):

$$-l_1 = \frac{l_2}{2} = \frac{\hbar cd}{2e^2\tau}, \quad (5.11a)$$

$$\frac{\lambda}{l_3(0)l_4} = \frac{3e^2\tau}{4\hbar cd}. \quad (5.11b)$$

Now we may express the results for the two cases discussed in the last section in terms of the microscopic parameters. The Hall voltage induced by an external current is found to be

$$V_H = eI \frac{\hbar}{16(ek_F\lambda)^2} \left(2\kappa + \frac{3\kappa}{\kappa+1}\right) \quad (5.12)$$

in the leading order in τ . Here we have made use of the relation $(k_F\lambda)^2 = mc^2 d/4e^2\tau$. We find a strong reduction compared with the quantum unit of resistance $R_0 = \hbar/2e^2$. The factor $1/(k_F\lambda)^2$ can be also written as $16\pi n_s\chi/n_0$, where n_s is the superfluid density and $\chi = \mu_B^2 N(0) = 3\chi_{\text{orb}}$ corresponding to the orbital susceptibility. We can thus rewrite Eq. (5.12) as

$$V_H = eI \frac{\pi\hbar\gamma\chi}{e^2} \left(2\kappa + \frac{3\kappa}{\kappa+1}\right), \quad (5.13)$$

where $\gamma = n_s/n_0 = 2\tau$ is the ratio of the superfluid density to the electron density. Obviously the Hall resistance strongly depends on material dependent parameters and is also rather severely reduced from the universal value \hbar/e^2 . In Sec. VI we will analyze the quantitative aspect in more detail.

We turn now to the reciprocal case (2). Here the effect is more subtle as the response to an external electric field constitutes a change of the field distribution in the vicinity of the surface. Since there is already spontaneous magnetization generated by the surface currents, we estimate the relative change of the total magnetic flux

$$\frac{\delta\Phi}{\Phi^{(0)}} = \frac{\delta A_y^{(2)}(0)}{A_y^{(0)}(0)} = -\frac{eEl^2}{\mu\lambda} \left(\kappa + \frac{5}{2}\right). \quad (5.14)$$

The electric field E should be smaller than Δ/el in order to avoid nonlinear effects that arise from the field effect on the superconducting order parameter at the surface. Therefore the induced change of flux $\delta\Phi$ would only be a very small fraction of the spontaneous magnetic flux $\Phi^{(0)}$.

VI. DISCUSSION BASED ON HYDRODYNAMIC EQUATIONS

A. The hydrodynamic equations

In the previous sections we have considered the SHE using the self-consistent solution of the BdG equation at T

$=0$ and the extended GL theory near T_c . In this section we introduce a phenomenological description based on the stationary hydrodynamic equations. This approach can provide an interpolation between the two limits and allow us to have a simple intuitive understanding of the physics involved. Our starting point is the phenomenological Lagrangian

$$F = \int d^3r \left[f + eA_0 \frac{\partial f}{\partial \mu} - \frac{1}{8\pi} (\nabla A_0)^2 - \frac{1}{8\pi l^2} A_0^2 + \frac{1}{8\pi} (\nabla \times \mathbf{A})^2 \right], \quad (6.1)$$

which describes electromagnetic properties of a superconductor. In the chiral p -wave state the Lagrangian density f may be written as

$$f = n_s \left[\frac{m}{2} (\mathbf{v}_s + \mathbf{v}_0)^2 + \nabla \cdot (\boldsymbol{\mu} \times \mathbf{A}) \right], \quad (6.2)$$

where $\mathbf{v}_s = (e/mc)\mathbf{A}$ and \mathbf{v}_0 is the velocity of the supercurrent generated by the spatial dependence of the order parameter

$$\mathbf{v}_0 = \begin{pmatrix} v_{0x} \\ v_{0y} \end{pmatrix} = \frac{\hbar}{8m\eta_0^2} \left[\begin{pmatrix} \text{Im}(3\eta_x^* \partial_x \eta_x + \eta_y^* \partial_x \eta_y) \\ \text{Im}(3\eta_y^* \partial_y \eta_y + \eta_x^* \partial_y \eta_x) \end{pmatrix} + \begin{pmatrix} \text{Im}(\eta_x^* \partial_y \eta_y + \eta_y^* \partial_y \eta_x) \\ \text{Im}(\eta_x^* \partial_x \eta_y + \eta_y^* \partial_x \eta_x) \end{pmatrix} \right]. \quad (6.3)$$

The first term corresponds to the ordinary supercurrent due to phase gradient, while the second term is connected with the spontaneous current due to texture of the order parameter. The latter is equivalent to the surface current of the chiral edge states and will be important for our discussion. The partial derivative in Eq. (6.1) acts on n_s as

$$\frac{\partial n_s}{\partial \mu} = \frac{\partial n_s}{\partial n_0} \frac{\partial n_0}{\partial \mu} = 2\gamma N(0), \quad (6.4)$$

where $\gamma = n_s/n_0$ is the ratio of the superfluid density n_s to the electron density $n_0 = k_F^2/2\pi d$. We know the two limiting values of γ : $\gamma=1$ at $T=0$ and $\gamma=2\tau$ near T_c .

The Lagrangian density f can be deduced from the GL Lagrangian in the following way. In the chiral p -wave state we may assume without loss of generality that $\eta_x^* \eta_y$ is imaginary. With the weak-coupling result (5.4c), it is easy to confirm that the K_i terms in \mathcal{F} (3.2) generate $n_s m \mathbf{v}_s \cdot \mathbf{v}_0$, in addition to $n_s (m/2) \mathbf{v}_s^2$. The latter term can be obtained with the approximation $|\eta_x|^2 = |\eta_y|^2 = \eta_0^2$. It is then natural to complete the square to make $m(\mathbf{v}_s + \mathbf{v}_0)^2/2$, which is nothing but the kinetic energy of the superfluid in the presence of the spontaneous flow with the velocity \mathbf{v}_0 . From the relation $\tilde{K}_i = e \partial K_i / \partial \mu$, one can also see that the \tilde{K}_i terms lead to the kinetic energy contribution to $eA_0 \partial f / \partial \mu$. Furthermore, we find from Eqs. (3.4) and (5.10c) that the C_i terms have a contribution

$$\begin{aligned} & -iC_1 \frac{8e}{\hbar c} \int d^3r (\eta_x^* \eta_y - \eta_y^* \eta_x) (A_y \partial_x A_0 - A_x \partial_y A_0) \\ & = iC_1 \frac{8e}{\hbar c} \int d^3r A_0 \nabla \cdot [\mathbf{A} \times \hat{\mathbf{z}} (\eta_x^* \eta_y - \eta_y^* \eta_x)] \\ & \quad + \text{surface term} \end{aligned} \quad (6.5)$$

in the chiral p -wave state where $\eta_x^* \eta_y$ is imaginary. This gives the remaining term $2\gamma e A_0 N(0) n_s \nabla \cdot (\boldsymbol{\mu} \times \mathbf{A})$. With the help of the identity $\nabla \cdot (\boldsymbol{\mu} \times \mathbf{A}) = \mathbf{A} \cdot (\nabla \times \boldsymbol{\mu}) - \boldsymbol{\mu} \cdot (\nabla \times \mathbf{A})$, we find that $\nabla \cdot (\boldsymbol{\mu} \times \mathbf{A})$ represents the coupling of the magnetic current $\nabla \times \boldsymbol{\mu}$ to the vector potential as well as the Zeeman energy of the magnetic moment $\boldsymbol{\mu}$. It is important to realize that the full magnetic moment of a chiral Cooper pair appears here, without reduction found in Eq. (5.5). The scalar potential induces a change in the number of Cooper pairs, which is necessarily accompanied by the change of the full magnetic moment per Cooper pair.²⁵

We now take the variation of F with respect to \mathbf{A} to obtain the extended London equation

$$\nabla^2 \mathbf{A} - \frac{1}{\lambda^2} \mathbf{A} + \frac{4\pi}{c} \mathbf{j} = 0, \quad (6.6)$$

with the current density

$$\mathbf{j} = -n_s e \mathbf{v}_0 - 2e\gamma N(0) [eA_0 (\mathbf{v}_s + \mathbf{v}_0) + c\mathbf{E} \times \boldsymbol{\mu}]. \quad (6.7)$$

The variation of F with respect to A_0 yields

$$\nabla^2 A_0 - \frac{1}{l^2} A_0 + \frac{8\pi e N(0)}{n_0} f = 0. \quad (6.8)$$

Since the Thomas-Fermi screening length l is much shorter than ξ and λ , we may ignore $\nabla^2 A_0$ to obtain immediately

$$A_0 = \frac{n_s}{en_0} \left[\frac{m}{2} (\mathbf{v}_s + \mathbf{v}_0)^2 + \nabla \cdot (\boldsymbol{\mu} \times \mathbf{A}) \right], \quad (6.9)$$

which we may call a generalized Bernoulli equation. The first term represents a Bernoulli force coming from the kinetic energy of superfluid. In conventional superconductors without broken time-reversal symmetry, the spontaneous current is absent. In such a case a supercurrent I injected from an external current source can generate a transverse potential difference proportional to I^2 .^{29–31} On the other hand, in the case of our interest where a spontaneous current flows along a boundary ($\mathbf{v}_0 \neq 0$), an external current can induce a transverse potential difference proportional to I . The second term in Eq. (6.9) is characteristic of the chiral p -wave state where Cooper pairs have their magnetic moment. Both terms are important in the SHE and in its reciprocal effect.

B. Spontaneous Hall effect and its reciprocal effect

Let us study the spontaneous Hall effect using the hydrodynamic equations. As in Sec. IV, we consider a chiral p -wave superconductor with a boundary at $x=0$ only. The superconductor occupies the positive x region and the system is translationally invariant in the y and z directions. We sup-

pose that the spatial profile of the order parameter $\boldsymbol{\eta}(\mathbf{r}) = (\eta_x(x), \eta_y(x))$ is already determined self-consistently in the equilibrium state. In particular, as we have observed in the BdG calculation in Sec. II, the order parameter satisfies $\eta_x = d\eta_y/dx = 0$ at $x=0$ under the assumption of the specular reflection at the surface. We will calculate a linear response to weak electromagnetic perturbation.

The local variation of $\boldsymbol{\eta}$ near the boundary yields a spontaneous current due to the order parameter texture $\mathbf{j}_t = -n_s e \mathbf{v}_t$, where

$$\mathbf{v}_t = \frac{\hbar}{8m\eta_0^2} \text{Im} \left(\eta_x^* \frac{d\eta_y}{dx} + \eta_y^* \frac{d\eta_x}{dx} \right) \hat{\mathbf{y}}. \quad (6.10)$$

This current determines the vector potential $\mathbf{A} = (0, A_y, 0)$ obeying the London equation

$$\left(\frac{d^2}{dx^2} - \frac{1}{\lambda^2} \right) \mathbf{A} = -\frac{4\pi}{c} \mathbf{j}_t, \quad (6.11)$$

whose solution under the boundary condition $\partial_x A_y = 0$ at $x = 0$ is

$$A_y^{(0)}(x) = \frac{2\pi\lambda}{c} \int_0^\infty (e^{-|x-x'|/\lambda} + e^{-|x+x'|/\lambda}) \mathbf{j}_t(x') dx'. \quad (6.12)$$

In particular, its boundary value is

$$A_y^{(0)}(0) = \frac{\pi n_s \lambda \mu_B}{\eta_0^2} \int_0^\infty e^{-x/\lambda} \text{Im} \left(\eta_x \frac{d\eta_y^*}{dx} + \eta_y \frac{d\eta_x^*}{dx} \right) dx. \quad (6.13)$$

Having determined $\boldsymbol{\eta}$ and \mathbf{A} , we are now ready to obtain the scalar potential A_0 from the generalized Bernoulli equation.

Suppose that a small current I is injected from an external source to the superconductor, yielding a small change in the vector potential $\mathbf{A} = \mathbf{A}^{(0)} + \delta\mathbf{A}$, where $\delta\mathbf{A}(0) = -I(2\pi\lambda/cd)\hat{\mathbf{y}}$. Accordingly, the scalar potential acquires a small change, whose boundary value is

$$\delta A_0(0) = \frac{n_s}{en_0} \delta\mathbf{A} \cdot \left(\frac{e^2}{mc^2} \mathbf{A}^{(0)} + \frac{e}{c} \mathbf{v}_t + \nabla \times \boldsymbol{\mu} \right) \Big|_{x=0}, \quad (6.14)$$

where we have used the fact that $\boldsymbol{\mu} = 0$ at $x = 0$. The intrinsic magnetic moment $\boldsymbol{\mu}$ defined in Eq. (5.6) gives

$$\nabla \times \boldsymbol{\mu} = \frac{\mu_B}{2\eta_0^2} \text{Im} \left(\frac{d\eta_x^*}{dx} \eta_y + \eta_x^* \frac{d\eta_y}{dx} \right) \hat{\mathbf{y}}. \quad (6.15)$$

The spontaneous Hall voltage in the Hall bar geometry can be related to δA_0 by the relation $V_H = -2\delta A_0(0)$ as in Sec. IV. From Eqs. (6.10), (6.12), and (6.15) we obtain

$$\frac{V_H}{I} = \frac{2\pi\hbar n_s \chi}{e^2 n_0 \eta_0^2} \left[\lambda \text{Im} \left(\eta_y \frac{d\eta_x^*}{dx} \right) \Big|_{x=0} + \int_0^\infty e^{-x/\lambda} \text{Im} \left(\eta_x \frac{d\eta_y^*}{dx} + \eta_y \frac{d\eta_x^*}{dx} \right) dx \right]. \quad (6.16)$$

With the approximate form (4.5) of the order parameter used in Sec. IV, Eq. (6.16) becomes

$$\frac{V_H}{I} = \varepsilon \gamma \chi \frac{2\pi\hbar}{e^2} \left(\kappa + \frac{\kappa}{\kappa+1} \right) \quad (6.17)$$

which compares well with Eq. (5.13).

The quantitative comparison with the self-consistent solution of the BdG equations encounters some drawback from the fact that for the sake of numerical accuracy the cutoff energy ω_c had to be taken comparable to the Fermi energy. Therefore, there are larger strong-coupling corrections not included in our phenomenological analysis. Nevertheless, we find a reasonably good agreement between the phenomenological and the BdG estimates. The result from the numerical BdG calculation ($k_F \xi_0 = 16$ and $l/\xi_0 = 0.1$) is

$$\frac{V_H}{I} \approx \frac{h}{2e^2} \times 10^{-3} \times \begin{cases} 1.3, & \kappa = 1 \\ 0.5, & \kappa = 2, \end{cases} \quad (6.18)$$

while Eq. (6.17) with the same parameters (apart from ω_c) leads to

$$\frac{V_H}{I} \approx \frac{h}{2e^2} \times 10^{-3} \times \begin{cases} 1.5, & \kappa = 1 \\ 0.65, & \kappa = 2. \end{cases} \quad (6.19)$$

The discrepancy is not only a result of weak-coupling versus strong-coupling approach, but we would like to remind that we have also used an approximate description of the order parameter texture at the surface.

Obviously the resistance obtained here is considerably smaller than the universal unit h/e^2 . Now we would like to build a connection between the SHE and the ordinary Hall effect. We may look for the intrinsic magnetic field which causes the Hall response to the externally induced current I . Comparing Eq. (6.17) with the standard expression of the Hall effect

$$V_H = \frac{1}{n_0 e c} \frac{I H_{\text{eff}}}{d}, \quad (6.20)$$

we obtain the effective magnetic field

$$H_{\text{eff}} = \pi n_s \mu_B \kappa \left(1 + \frac{1}{1+\kappa} \right). \quad (6.21)$$

The effective field corresponds to the density of magnetic moments of Cooper pairs which is not the reduced magnetic moment in Eq. (5.5), but rather the full moment which is associated with the change of the Cooper pair density. Note that the factor $\pi\kappa[1 + 1/(1+\kappa)]$ is due to inhomogeneous field and current distribution.

Next we consider the reciprocal effect. In the presence of a weak external electric field $\delta\mathbf{E} = E\hat{x}$ at $x < 0$, the scalar potential in the superconductor receives a small perturbation $\delta A_0(x) = E l e^{-x/l}$. This yields a small change in the current density

$$\begin{aligned}\delta\mathbf{j}(x) &= -2e\gamma N(0) \left[e\delta A_0 \left(\mathbf{v}_t + \frac{e}{mc} \mathbf{A}^{(0)} \right) + c\delta\mathbf{E} \times \boldsymbol{\mu} \right] \\ &= -2ce\gamma N(0) E e^{-x/l} \left[l \left(\frac{e}{c} v_{ty} + \frac{e^2}{mc^2} A_y^{(0)} \right) - \mu_z \right] \hat{y},\end{aligned}\quad (6.22)$$

which determines the change in the vector potential $\delta\mathbf{A}$. Solving the London equation, we find

$$\delta A_y(0) = \frac{4\pi\lambda}{c} \int_0^\infty e^{-x/\lambda} \delta j_y(x) dx. \quad (6.23)$$

Since the Thomas-Fermi screening length l is much shorter than ξ and λ , we may set $v_{ty}(x) = v_{ty}(0)$, $A_y^{(0)}(x) = A_y^{(0)}(0)$, and $\mu_z(x) = x\mu'_z(0)$ in $\delta j_y(x)$ in the integrand. With this approximation we obtain

$$\begin{aligned}\delta A_y(0) &= -E \frac{\gamma\lambda}{e} \left(\frac{e}{c} v_{ty} + \frac{e^2}{mc^2} A_y^{(0)} - \frac{d\mu_z}{dx} \right) \Big|_{x=0} \\ &= -E \frac{n_s \mu_B}{4en_0 \eta_0^2} \left[\lambda \text{Im} \left(\eta_y \frac{d\eta_x^*}{dx} \right) \Big|_{x=0} \right. \\ &\quad \left. + \int_0^\infty e^{-x/\lambda} \text{Im} \left(\eta_x \frac{d\eta_y^*}{dx} + \eta_y \frac{d\eta_x^*}{dx} \right) dx \right].\end{aligned}\quad (6.24)$$

The magnitude of the ratio $\delta A_y(0)/A_y^{(0)}(0)$ may be estimated from Eqs. (6.13) and (6.24) for the approximate form (4.5), yielding

$$\frac{\delta A_y(0)}{A_y^{(0)}(0)} = -\frac{eEl^2}{\mu\lambda} (\kappa + 2), \quad (6.25)$$

in good agreement with the GL analysis. Unfortunately, in this case the comparison with the BdG result does not agree well, which we attribute to the fact that l is comparable to the other length scales in the numerical calculation. Thus, there are strong corrections to the above result in addition to the strong-coupling corrections.

C. Experimental probe

Although the phenomenon we discuss in this paper can be compared to the standard Hall effect, it has actually some quite distinct aspects. Flowing currents are an equilibrium property of the superconductor. It is, therefore, impossible to measure the transverse voltage by means of standard voltmeters, using direct contacts to the surfaces. This problem was realized already more than 30 years ago, when the Bernoulli response to a current was investigated in conventional superconductors.³² In this case a potential difference between

the surface and the interior of the superconductor is expected, which is proportional to the square of the running current

$$V = \frac{2\pi}{ec^2 d^2 n_0} I^2. \quad (6.26)$$

The potential difference is actually independent of temperature as has been observed³² for Pb. The method of measurement was based on a thin-film capacitor which picks up the voltage signal caused by an ac-current on the superconductor surface. The same kind of capacitor technique could also be used to detect the spontaneous Hall effect. In an ac-measurement the above Bernoulli force ($\propto I^2$) yields the second harmonic of the applied ac-current, while the signal corresponding to the SHE ($\propto I$) contributes to the first harmonic. Hence we can distinguish the SHE from the standard Bernoulli effect. We can estimate the magnitude of the Hall response

$$V_H = R_H I = \frac{R_H I_{\text{tot}}}{N_{\text{layer}}} \approx \frac{h}{4e^2} \frac{1}{k_F^2 \lambda^2} \frac{I_{\text{tot}}}{N_{\text{layer}}}, \quad (6.27)$$

where I_{tot} is the total current running through a three-dimensional sample consisting of N_{layer} layers. Using typical values for ordinary metals (for example, $k_F \lambda \approx 200$ at $T = 0$), we obtain $R_H \approx 0.16\Omega$. If $I_{\text{tot}}/N_{\text{layer}} = 1$ nA, then we expect $V_H \approx 0.16$ nV, which might be experimentally accessible. Under the same conditions the conventional Bernoulli signal is considerably smaller, $V \sim 1$ pV. It is worth noting that the capacitor technique in measuring the transverse potential change does not require a Hall bar geometry, but a single surface is sufficient.

Unfortunately, in addition to the high sensitivity necessary in this kind of measurements a further problem has to be taken into account. This is the formation of domains of degenerate superconducting states with opposite chiralities. Such domain formation is very likely to occur when a system enters the superconducting state. The two domains with opposite chiralities yield opposite sign of the transverse voltage so that the net effect might be diminished. Since the spontaneous Hall voltage is a surface effect, the number of domain walls intersecting the surface matters. It would be necessary to establish an experimental technique to realize a single domain phase, for example, by cooling in a weak magnetic field.

VII. NONCHIRAL TIME-REVERSAL SYMMETRY BREAKING STATES

We now consider the possibility of a spontaneous Hall effect in nonchiral time reversal symmetry breaking superconductors. While for these superconducting states there is no anomalous CS-like coupling between scalar and vector potential, there are still spontaneous surface currents for certain orientations of the sample boundaries, despite the fact that the Cooper pairs do not have a net angular momentum. These surface currents can be associated with Andreev bound states. Thus we would expect at least to find a contribution to the SHE due to the Bernoulli force. We consider

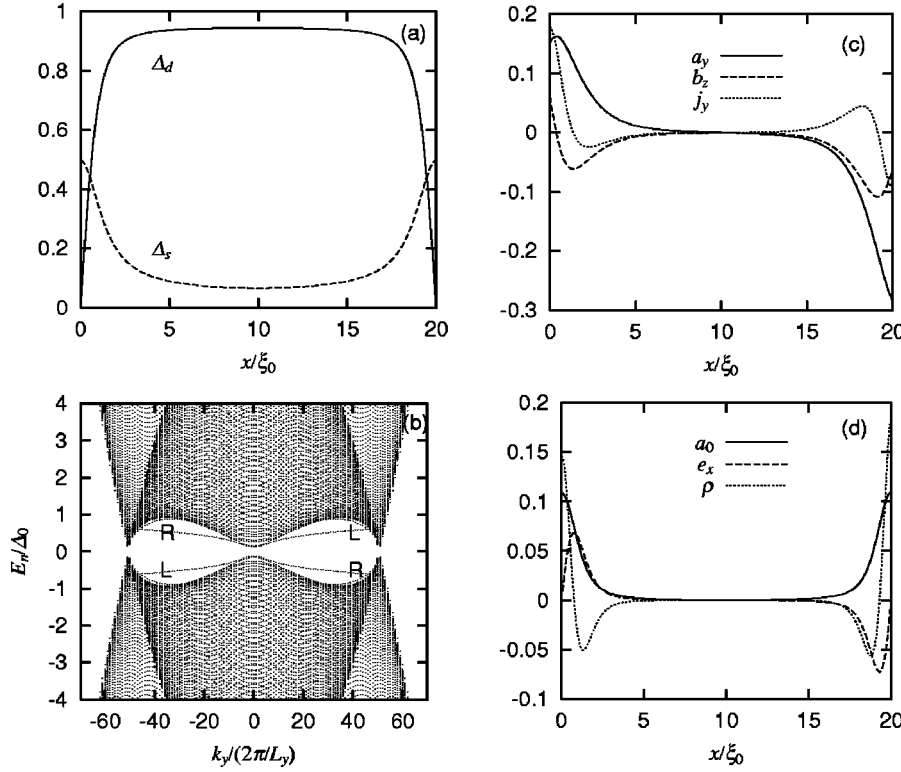


FIG. 4. Self-consistent solution of the Bogoliubov-de Gennes equation for the [100] surface in the $d_{xy} + is$ -wave state at $T=0$. The set of parameters are the same as used in Fig. 2. (a) Order parameter scaled by Δ_0 , which is the magnitude of the order parameter for the d_{xy} wave in the bulk region. Δ_d and Δ_s are the magnitude of the order parameter of the d_{xy} wave and s wave, respectively. (b) Energy eigenvalues obtained for sine basis functions. L and R denote the surface bound states localized near left and right side surfaces, respectively. (c) Dimensionless vector potential $a_y = (e\xi_0/\hbar c)A_y$, magnetic field $b_z = \xi_0\partial_x a_y$, and current density $j_y = -\xi_0\partial_x b_z$. Total current is $I = 5e\Delta_0/\hbar k_F \xi_0$. (d) Dimensionless scalar potential $a_0 = eA_0/\Delta_0$, electric field $e_x = -\xi_0\partial_x a_0$, and charge density $\rho = \xi_0\partial_x e_x$.

one of the well-known examples of a nonchiral superconducting state in a quasi-two-dimensional system that violates time-reversal symmetry, the $d + is$ -wave state. We assume that the d -wave state has the d_{xy} symmetry, for which a spontaneous surface current runs along surfaces normal to the [100] or [010] direction.³³ It is possible here to express the spontaneous current again as a result of the order parameter texture analogous to Eq. (6.3):

$$\mathbf{v}_0 = \begin{pmatrix} v_{tx} \\ v_{ty} \end{pmatrix} = \frac{\hbar}{8m\eta_0^2} \begin{pmatrix} \text{Im}(\eta_s^* \partial_y \eta_d + \eta_d^* \partial_y \eta_s) \\ \text{Im}(\eta_s^* \partial_x \eta_d + \eta_d^* \partial_x \eta_s) \end{pmatrix}, \quad (7.1)$$

where η_s and η_d denote the order parameters of the s -wave and d -wave component, respectively. The currents can be of similar magnitude as for the chiral p -wave state and consequently the size of the SHE is comparable. There are, of course, some differences from the former case. Since the two pairing components are not degenerate in general, various additional parameters may appear in the discussion. We have performed a BdG calculation for a specific set of parameters to verify the expectation of the above argument.

Figure 4 shows the data obtained from the self-consistent solution of the BdG equation for the $(d_{xy} + is)$ -wave state at zero temperature. Here we present the results for the case where a finite net current is running in the system. Again the order parameter shows strong variation at the surface, whereby the d -wave component is suppressed and the s -wave component enhanced [Fig. 4(a)]. Looking at the quasiparticle spectrum in Fig. 4(b), we see obvious differences between the chiral and the nonchiral cases. In both cases there are Andreev bound states below the ordinary continuous spectra of scattering states. In the nonchiral case, however, there is no gapless edge mode, in accordance with the expectation

from the index theorem. The electromagnetic properties in the Hall bar geometry, shown in Figs. 4(c) and 4(d), are very similar to the chiral case. Also, the Hall resistance R_H for the parameters indicated in the figure caption is of similar magnitude. We thus conclude that for certain surface orientations the measurement of the transverse voltage in a nonchiral state gives a qualitatively identical result to a chiral state. Hence, experiments of this kind on the [110] surface of high-temperature superconductors, where a low-temperature time-reversal symmetry breaking phase may be present, would not be able to give decisive results as to which state is realized, the nonchiral $d_{x^2-y^2} + is$ -wave state or the chiral $d_{x^2-y^2} + id_{xy}$ -wave state.

VIII. CONCLUSIONS

We have analyzed in detail the spontaneous Hall effect in time reversal symmetry breaking quasi-two-dimensional superconductor of chiral and nonchiral nature. There are two contributions to the SHE. One is connected with the Bernoulli (or Lorentz) force due to the presence of spontaneous surface currents. The other originates from the presence of an orbital angular momentum of Cooper pairs. While the former contribution appears in both types of superconducting states, there is no angular momentum in the nonchiral case. We have shown in our phenomenological treatment that the angular momentum gives rise to a Chern-Simons-like term in the Lagrangian determining the electromagnetism of the superconductor, similar to derivations based on topological arguments.^{9,19} Although it was suggested that the Hall response would be, at least, close to a universal value, our analysis shows that the actual measurement of the Hall voltage gives a considerably smaller nonuniversal value. Nevertheless, the comparison of the SHE with the ordinary Hall

effect reveals the presence of an intrinsic effective magnetic field corresponding to the density of Cooper pair magnetic moments.

The effect depends on the presence of spontaneous surface currents. In our analysis we have restricted ourselves to the case of a perfect, specularly scattering surface. Rough surfaces with diffuse scattering would reduce the spontaneous currents and the Hall voltage. Moreover, domain formation constitutes another obstacle to the measurement of the SHE, because different domains give contributions of opposite signs. Nevertheless, we believe that experimental techniques available at present are sufficiently accurate to observe the spontaneous Hall effect.

ACKNOWLEDGMENTS

We thank Y. Maeno, K. Deguchi, K. Ishikawa, J. Goryo, and V. Yakovenko for stimulating discussions. The work of A.F. and M.S. was supported in part by Grant-in-Aid for Scientific Research on Priority Areas (A) from The Ministry of Education, Science, Sports and Culture (Grant No. 12046238) and by Grant-in-Aid for Scientific Research (C) from Japan Society for the Promotion of Science (Grant No. 10640341). The work of M.M. was supported by a Grant-in-Aid for Encouragement of Young Scientists from Japan Society for the Promotion of Science (Grant No. 10740169) and by the Casio Science Promotion Foundation.

*Permanent address: Theoretische Physik, ETH-Hönggerberg, CH-8093 Zurich, Switzerland.

¹G. E. Volovik and L. P. Gor'kov, JETP Lett. **39**, 674 (1984); Sov. Phys. JETP **61**, 843 (1985).

²M. Matsumoto and H. Shiba, J. Phys. Soc. Jpn. **64**, 3384 (1995); **64**, 4867 (1995); **65**, 2194 (1996).

³M. Fogelström, D. Rainer, and J. A. Sauls, Phys. Rev. Lett. **79**, 281 (1997).

⁴M. Sigrist, Prog. Theor. Phys. **99**, 899 (1998).

⁵R. H. Heffner and M. R. Norman, Comments Condens. Matter Phys. **17**, 361 (1996).

⁶Y. Maeno, H. Hashimoto, K. Yoshida, S. Nishizaki, T. Fujita, J. G. Bednorz, and F. Lichtenberg, Nature (London) **372**, 532 (1994).

⁷T. M. Rice and M. Sigrist, J. Phys.: Condens. Matter **7**, L643 (1995); G. Baskaran, Physica B **223-224**, 490 (1996).

⁸A. J. Leggett, Rev. Mod. Phys. **47**, 331 (1975).

⁹G. E. Volovik, Sov. Phys. JETP **67**, 1804 (1988).

¹⁰G. E. Volovik, JETP Lett. **66**, 522 (1997).

¹¹G. M. Luke, Y. Fudamoto, K. M. Kojima, M. I. Larkin, J. Merrin, B. Nachumi, Y. J. Uemura, Y. Maeno, Z. Q. Mao, Y. Mori, H. Nakamura, and M. Sigrist, Nature (London) **394**, 558 (1998).

¹²K. Ishida, H. Mukuda, Y. Kitaoka, K. Asayama, Z. Q. Mao, Y. Mori, and Y. Maeno, Nature (London) **396**, 658 (1998).

¹³M. Sigrist, D. Agterberg, A. Furusaki, C. Honerkamp, K. K. Ng, T. M. Rice, and M. E. Zhitomirsky, Physica C **317-318**, 134 (1999).

¹⁴L. J. Buchholtz and G. Zwirnagel, Phys. Rev. B **23**, 5788 (1981).

¹⁵M. Yamashiro, Y. Tanaka, and S. Kashiwaya, Phys. Rev. B **56**, 7847 (1997).

¹⁶C. Honerkamp and M. Sigrist, J. Low Temp. Phys. **111**, 895 (1998).

¹⁷M. Matsumoto and M. Sigrist, J. Phys. Soc. Jpn. **68**, 994 (1999).

¹⁸F. Laube, G. Goll, H. v. Löhneysen, M. Fogelström, and F. Lichtenberg, Phys. Rev. Lett. **84**, 1595 (2000).

¹⁹J. Goryo and K. Ishikawa, Phys. Lett. A **260**, 294 (1999).

²⁰T. Senthil, J. B. Marston, and M. P. A. Fisher, Phys. Rev. B **60**, 4245 (1999).

²¹N. Read and D. Green, Phys. Rev. B **61**, 10 267 (2000).

²²G. E. Volovik and V. M. Yakovenko, J. Phys.: Condens. Matter **1**, 5263 (1989).

²³M. Sigrist and K. Ueda, Rev. Mod. Phys. **63**, 239 (1991).

²⁴V. P. Mineev and K. V. Samokhin, *Introduction to Unconventional Superconductivity* (Gordon and Breach, Amsterdam, 1999).

²⁵G. E. Volovik and V. P. Mineev, Sov. Phys. JETP **54**, 524 (1981).

²⁶M. C. Cross, J. Low Temp. Phys. **21**, 525 (1975); **26**, 165 (1977).

²⁷N. D. Mermin and P. Muzikar, Phys. Rev. B **21**, 980 (1980).

²⁸G. E. Volovik, JETP Lett. **61**, 958 (1995).

²⁹F. London, *Superfluids* (Wiley, New York, 1950), Vol. 1, Sec. B.

³⁰A. G. Van Vijfeijken and F. A. Staas, Phys. Lett. **12**, 175 (1964).

³¹G. Rickayzen, J. Phys. C **2**, 1334 (1969).

³²T. D. Morris and J. B. Brown, Physica (Amsterdam) **55**, 760 (1971).

³³This is equivalent to the $d_{x^2-y^2} + is$ -wave case for the [110] surfaces.